DOI: 10.1002/chem.201102210

Intramolecular [2+2+2] Cycloaddition Reactions of Yne-ene-yne and Yne-yne-ene Enediynes Catalysed by Rh^I: Experimental and Theoretical Mechanistic Studies

Anna Dachs,[a, b] Anna Pla-Quintana,[a] Teodor Parella,[c] Miquel Solà,*[a, b] and Anna Roglans*[a]

In memory of Professor Rafael Suau

Abstract: *N*-Tosyl-linked open-chain yne-ene-yne enediynes **1** and **2** and yne-yne-ene enediynes **3** and **4** have been satisfactorily synthesised. The [2+2+2] cycloaddition process catalysed by the Wilkinson catalyst [RhCl-$(PPh_3)_3$] was tested with the above-mentioned substrates resulting in the production of high yields of the cycloadducts. Enediynes **1** and **2** gave standard [2+2+2] cycloaddition reactions whereas enediynes **3** and **4** suffered β-hydride elimination followed by reductive elimination of the Wilkinson catalyst to give cycloadducts, which are isomers of those that would be obtained by standard [2+2+2] cycloaddition reactions. The different reactivities of these two types of enediyne have been rationalised by density functional theory calculations.

Keywords: cycloaddition · density functional calculations · enediynes · reaction mechanisms · rhodium

Introduction

The transition-metal-catalysed [2+2+2] cycloaddition reactions of moieties consisting of two alkynes and an alkene are a well-established method for the synthesis of 1,3-cyclohexadienes. Several transition-metal complexes have been reported as efficient catalysts in this process.[1–3] Among them, rhodium catalysts are becoming increasingly popular[4] especially in the enantioselective reaction in which [2+2+2] cycloaddition reactions of diynes and alkenes,[5] enynes and alkynes,[6] and enediynes[7] have been reported.

Recently, Saá and co-workers studied the cycloaddition reactions of α,ω-diynes with alkenes by using a ruthenium complex as catalyst to give cyclohexadiene products.[8] With cyclic alkenes, the standard [2+2+2] cycloaddition pathway prevailed, leading to 1,3-cyclohexadienes of type **A** (Scheme 1). However, when the alkene moiety was acyclic, cyclohexadienes of type **C** were obtained. DFT calculations identified a common ruthenacycloheptadiene intermediate (**I**) from which the two final products arose by either reductive elimination (product **A**) or β-hydride elimination followed by a reductive elimination (product **B**). In the latter case, the 1,3,5-triene (**B**) suffered a thermal disrotatory $6e^-$ π electrocyclisation to afford cyclohexadiene derivative **C**.

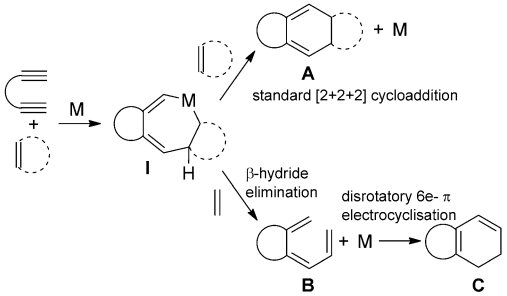

Scheme 1. Two possible reaction pathways for the cycloaddition reactions of diynes and alkenes

In agreement with the discovery of this new reaction pathway, Aubert, Gandon and co-workers[9] reported the cycloaddition reactions of diynes with enol ethers catalysed by stoichiometric $[CpCoL_2]$ (Cp = cyclopentadienyl).[9a] DFT calculations confirmed that the energy barriers of the [2+2+2] reductive and β-hydride elimination pathways are similar, in line with previous results obtained by the same authors.[9b]

[a] Dr. A. Dachs, Dr. A. Pla-Quintana, Prof. M. Solà, Prof. A. Roglans
Departament de Química, Universitat de Girona
Campus de Montilivi, s/n. 17071 Girona (Spain)
E-mail: miquel.sola@udg.edu
anna.roglans@udg.edu

[b] Dr. A. Dachs, Prof. M. Solà
Institut de Química Computacional, Universitat de Girona
Campus de Montilivi, s/n. 17071 Girona (Spain)

[c] Dr. T. Parella
Servei de RMN, Universitat Autònoma de Barcelona
08193 Cerdanyola, Barcelona (Spain)

Supporting information for this article is available on the WWW under http://dx.doi.org/10.1002/chem.201102210. It contains NMR spectra for compounds **1**–**4**, **10**, **11**, **14** and **15**, cartesian *xyz* coordinates and total energies for all stationary points located. It also contains Figures 4–13 in colour.

 © 2011 Wiley-VCH Verlag GmbH & Co. KGaA, Weinheim

In the case of rhodium complexes, Tanaka and co-workers observed the formation of a hepta-2,4,6-trienamide in a single case described in a footnote when they combined an alkenylamide with a 1,6-diyne in the presence of [Rh(cod)$_2$]BF$_4$/BIPHEP (BIPHEP = 2,2'-bis(diphenylphosphino)-1,1'-biphenyl).[10] In addition, Ojima and co-workers[11] reported the formation of fused tetracyclic compounds starting from enediynes and carbon monoxide by a Rh^I-catalysed [2+2+2+1] cycloaddition reaction, which gave a 1:1 mixture of regioisomers of the expected product and its diene-shifted regioisomers. The authors did not give any mechanistic explanation for the formation of the latter.

The aim of this work was to study the [2+2+2] cycloaddition reactions of a set of enediynes of type yne-ene-yne and yne-yne-ene (see below) catalysed by Rh^I (in particular with the Wilkinson complex [RhCl(PPh$_3$)$_3$]) and to analyse whether the reaction products are those that would be expected from a characteristic [2+2+2] cycloaddition reaction or are derived from atypical β-hydride elimination pathways leading to unconventional cyclohexadiene derivatives. To understand the experimental results obtained, theoretical calculations by using density functional theory (DFT) with a hybrid functional were performed.

Results and Discussion

Synthesis: First, we applied our experience in the allylation of sulfonamides to create macrocycles for the preparation of **1** and **3** and their *N*-Boc-protected derivatives **2** and **4**. Scheme 2 shows the synthetic approaches to both types of enediyne (yne-ene-yne types **1** and **2** and yne-yne-ene types **3** and **4**). In the two cases, the starting product was the bromopropargylic derivative **5**. We had previously prepared compounds **5**,[12a] **6**,[12b] **7**[12a] and **8**.[12a] The treatment of **6** with an excess of bromide **5** in the presence of potassium carbonate as base in acetonitrile at reflux resulted in enediyne **1** in a yield of 75%, which, with the elimination of the two Boc groups, gave derivative **2** in a yield of 98%. Trisulfonamide **8** was treated with the allylic bromide **9**[12b] in K_2CO_3 and heated at reflux in acetonitrile to give derivative **3** in a yield of 75%. Elimination of the only Boc group led to an almost quantitative yield of **4**.

Once the corresponding unsaturated substrates had been obtained, we studied their [2+2+2] cycloaddition reactions (Scheme 3 and Table 1). The [RhCl(PPh$_3$)$_3$] complex was used as it is simple, relatively inexpensive and commercially available.

When catalytic amounts of [RhCl(PPh$_3$)$_3$] (10% molar) were used in toluene at 100°C under anhydrous conditions, the expected compounds **10** and **11** were obtained in good yields (entries 1 and 2, Table 1). The simplicity of the ^{1}H and ^{13}C NMR spectra proved a symmetrical structure due to the presence of a C_2 axis. The *anti* disposition of the new CH_c–$CH_{c'}$ centres was established by taking into account the *trans* configuration of the original double bond in the starting compounds **1** and **2**, respectively, and the NOE data. The full characterisation of compounds **10** and **11** by 2D correlation NMR spectroscopy (see the Supporting Information) confirmed that the process proceeded as a standard [2+2+2] cycloaddition reaction.

COSY data for **11** (see the experimental ^{1}H and ^{13}C NMR chemical shifts for the ring moiety in Figure 1) confirmed that the hydrogen atoms of the methylene groups 1 and 12 of the open chains ($\delta = 3.37$ and 3.68 ppm) only couple with the amine NH proton ($\delta = 7.74$ ppm). Furthermore, the H_c/$H_{c'}$ atoms of the cyclohexadiene ring are not coupled to these methylenes, as was confirmed by HMBC data. NOE data were essential to determine the relative *anti* stereochemistry of the symmetrical centres in **10** and **11**, in which the H_c proton in compound **11** shows a substantial NOE effect on the two closely situated H_a and $H_{b'}$ protons. This behaviour confirmed the *anti* stereochemistry of the compounds as the *syn* structure for compounds **10** and **11** would have given a minimum NOE signal between the H_c and H_a/$H_{b'}$ protons.

The cycloaddition reactions of azaenediynes **3** and **4** (entries 3 and 4 in Table 1) were carried out in toluene at 85°C under anhydrous conditions. In these cases, complete analysis of the NMR spectra confirmed that the expected derivatives **12** and **13**, respectively, were not formed. The products resulting from these transformations were characterised as their isomers, compounds **14** and **15**, respectively (see Figure 2 for the complete assignment of **15**).

If the standard [2+2+2] cycloadduct **13** (R = H) had been formed, the ^{1}H and ^{13}C NMR spectra would have been expected to show certain features relating to compound symmetry. However, analysis and complete chemical shift assignment by 2D NMR techniques (see the Supporting Information) provided evidence of a nonsymmetric compound. Thus, COSY data confirmed that the different methylene groups 1 and 12 are only coupled to the amine NH protons ($\delta = 7.37$ and 7.58 ppm, respectively). A key feature of the results was the HMBC three-bond crosspeaks between the C12 and C10 positions. Moreover, two different protons H_c

Abstract in Catalan: *S'han preparat satisfactòriament una sèrie d'endiins de cadena oberta amb unitats N-tosil i amb diferents posicions dels triples enllaços en la cadena (**1** i **2**, amb els triples enllaços no consecutius; **3** i **4**, amb els triples enllaços consecutius). Aquests endiins s'han emprat com a substrats en processos de cicloaddició [2+2+2] catalitzats pel complex de Wilkinson [RhCl(PPh$_3$)$_3$] obtenint-se bons rendiments dels corresponents cicloadductes. Els endiins **1** i **2** donen una reacció de cicloaddició [2+2+2] estàndard mentre que els endiins **3** i **4** pateixen una β-eliminació d'hidrur seguida d'una eliminació reductora del catalitzador de Wilkinson generant els cicloadductes **14** i **15**, els quals són isòmers dels que s'obtindrien per una cicloaddició [2+2+2] estàndard. La diferent reactivitat d'aquest dos tipus d'endiins s'ha racionalitzat mitjançant càlculs teòrics basats en la teoria del funcional de la densitat.*

 © 2011 Wiley-VCH Verlag GmbH & Co. KGaA, Weinheim

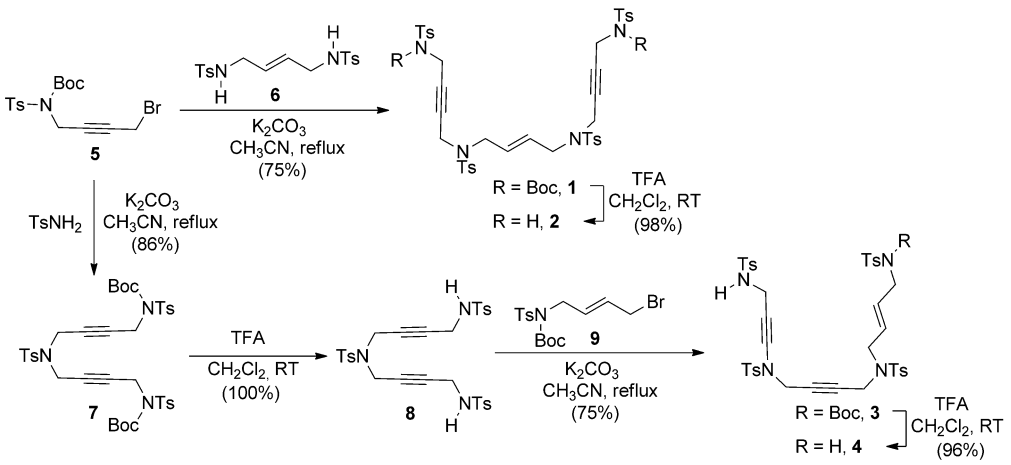

Scheme 2. Synthesis of enediynes **1–4** (TFA = trifluoroacetic acid; Ts = tosyl; Boc = *tert*-butyloxycarbonyl).

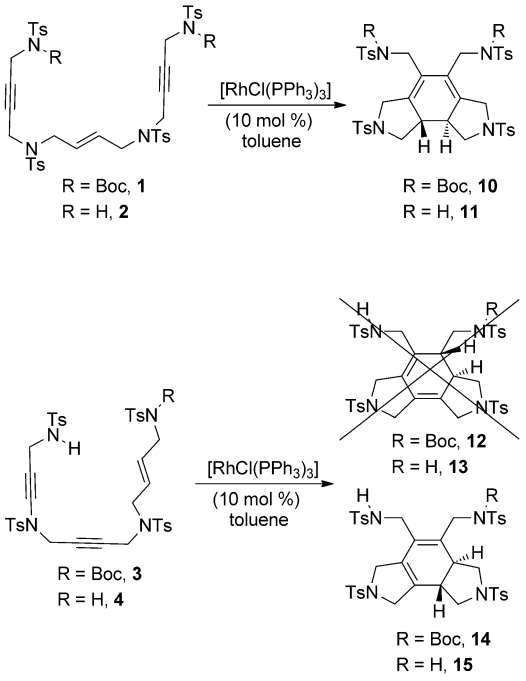

Scheme 3. Rh^{I}-catalysed cycloaddition reactions of compounds **1–4** to yield **10**, **11**, **14** and **15**.

Table 1. Rh^{I}-catalysed cycloaddition of compounds **1–4** to yield **10**, **11**, **14**, and **15**.

Entry	Enediyne	*T* [°C]	Reaction time [h]	Product (yield [%])
1	**1**	100	48	**10** (55)
2	**2**	100	48	**11** (85)
3	**3**	85	30	**14** (65)
4	**4**	85	28	**15** (89)

and H_d ($\delta = 2.73$ and 1.86 ppm, respectively) are coupled to each other and also to the corresponding vicinal CH_2 groups thereby confirming the presence of a CH_2–CH–CH–CH_2 spin system. NOE data were used to confirm the stereochemical assignments.

Computational calculations: Given the experimental results obtained, we performed B3LYP/cc-pVDZ-PP calculations (see the Computational Methods section for a more detailed description of the method used) to unravel the reaction mechanism of the intramolecular [2+2+2] cycloaddition reactions of the enediynes **1–4** catalysed by the Wilkinson complex (Scheme 3) to understand their different reactivities. To reduce the computational effort required, the tosyl moieties present in the experimental enediynes and the three phenyl groups of the Wilkinson catalyst were substituted by hydrogen atoms.[13,14] A previous study[15] with macrocyclic systems revealed that the substitution of the tosyl groups by hydrogen atoms reduces the exothermicity of the [2+2+2] cycloaddition by about 10%. Although this quantity is not negligible, we expect it to have only a slight effect on the different reaction mecha-

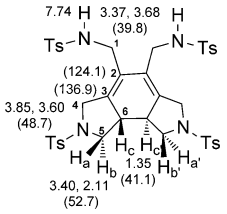

Figure 1. Selected ^{1}H and ^{13}C NMR chemical shifts (the latter in brackets) of **11** [ppm].

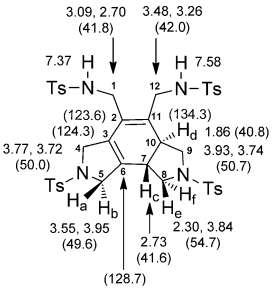

Figure 2. Selected ^{1}H and ^{13}C NMR chemical shifts (the latter in brackets) of **15** [ppm].

 © 2011 Wiley-VCH Verlag GmbH & Co. KGaA, Weinheim

nisms studied here and therefore the conclusions reached by our model systems will still be valid for experimental systems. Scheme 4 shows the model reactions studied in our theoretical calculations.

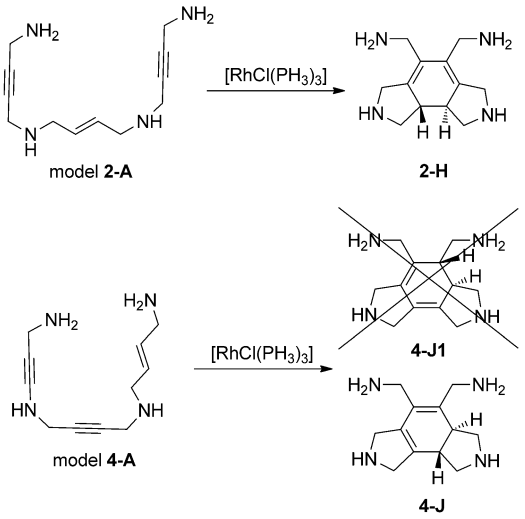

Scheme 4. Reaction models **2-A** and **4-A** for the Rh^{I}-catalysed cycloaddition reactions of compounds **1**–**4**.

*Yne-ene-yne enediynes **1** and **2***: We first examined the reaction mechanism for enediynes **1** and **2**, which were found to react by a standard [2+2+2] cycloaddition process. These two compounds differ in the protecting Boc groups on the terminal amines connected to the alkyne moieties, so we studied a model of these enediynes with terminal amines, model **2-A** in Scheme 4.

There are two possibilities for these enediynes in the initial C–C oxidative coupling step: either alkyne–alkyne coupling between two distant alkyne moieties or alkyne–alkene (enyne) coupling due to the coordination of the alkene and one alkyne moiety. In the latter, the alkene moiety has two different faces that can be coordinated (see Figure 3), so there are two possible enyne couplings.[16] The catalysis proceeds only if the Wilkinson catalyst loses one or two of the three initially coordinated phosphine ligands. Because both the resulting active species, $[RhCl(PH_3)_2]$ or $[RhCl(PH_3)]$, catalyse this oxidative coupling step, we have considered both possibilities.

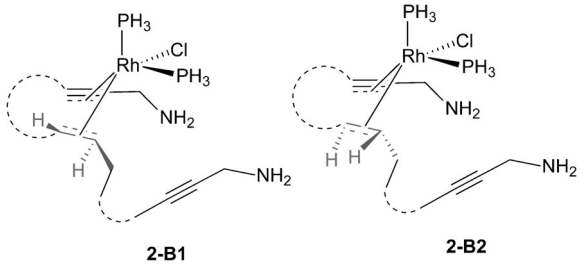

Figure 3. Schematic representation for the alkyne–alkene coordination (**2-B1** and **2-B2**) of rhodium with the two faces of the alkene moiety.

The three C–C oxidative couplings were analysed with the $[RhCl(PH_3)_2]$ catalytic species (Figure 4). Two of these couplings correspond to the coordination of alkene and alkyne moieties (**2-B1** and **2-B2**, Figure 3), yielding the distorted rhodacyclopentene adducts **2-C1** and **2-C2** via the transition states (TSs) **2-TS(B1,C1)** ($\Delta G^{\neq}=32.9$ kcal mol^{-1} with respect to **2-A** + $[RhCl(PH_3)_3]$) and **2-TS(B2,C2)** ($\Delta G^{\neq}=34.9$ kcal mol^{-1}), respectively. The third path, involving alkyne–alkyne coupling, transformed **2-B3** into **2-C3** via **2-TS(B3,C3)** with a barrier of $\Delta G^{\neq}=30.3$ kcal mol^{-1}. The small differences between the three Gibbs energy barriers indicate a competition between the three couplings, with the alkyne–alkyne coupling favoured, although only by about 3 kcal mol^{-1}.

The same three oxidative couplings were then studied with $[RhCl(PH_3)]$ as the catalytic species, that is, the species in which the rhodium retains only one PH_3 ligand (Figure 4). Enyne couplings with complexes **2-B4** and **2-B5** led to the rhodacyclopentene adducts **2-C4** and **2-C5** via **2-TS(B4,C4)** ($\Delta G^{\neq}=30.1$ kcal mol^{-1}) and **2-TS(B5,C5)** ($\Delta G^{\neq}=38.0$ kcal mol^{-1}), respectively. On the other hand, the alkyne–alkyne coupling step transformed **2-B** into **2-C** via **2-TS(B,C)** with $\Delta G^{\neq}=28.0$ kcal mol^{-1}.

Note that the preferred pathway is the alkyne–alkyne coupling when the rhodium has either one or two phosphine ligands attached, which have barriers of 28.0 and 30.3 kcal mol^{-1}, respectively. The small energy difference seems to indicate that both the reaction mechanisms via **2-TS(B,C)**, with the $[RhCl(PH_3)]$ catalytic species, and **2-TS(B3,C3)**, with the $[RhCl(PH_3)_2]$ catalyst, may be operative. Note, however, that the oxidative addition is both kinetically and thermodynamically favoured with the $[RhCl(PH_3)]$ catalytic species. In a previous study,[16] we analysed the oxidative coupling step for the same **2-A** system but with hydrogen and CH_3 groups instead of the CH_2–NH_2 groups as substituents on the alkyne moieties. For terminal alkynes (H instead of CH_2–NH_2), the barriers to the alkyne–alkyne coupling were 31.9 and 25.4 kcal mol^{-1} for the $[RhCl(PH_3)_2]$ and $[RhCl(PH_3)]$ catalysts, respectively, whereas in the case of alkynes with methyl groups, the barriers were higher; the $[RhCl(PH_3)_2]$ catalyst favoured the enyne coupling with $\Delta G^{\neq}=36.4$ kcal mol^{-1}, whereas the alkyne–alkyne coupling was preferred with the $[RhCl(PH_3)]$ catalyst with $\Delta G^{\neq}=32.6$ kcal mol^{-1}. On the whole, with H, CH_3 and CH_2–NH_2 in the enediynes of type **2-A**, the alkyne–alkyne coupling with the lowest barrier corresponds to the terminal alkynes with the $[RhCl(PH_3)]$ catalyst ($\Delta G^{\neq}=25.4$ kcal mol^{-1}) and to the CH_2–NH_2 substituent with the $[RhCl(PH_3)_2]$ catalyst ($\Delta G^{\neq}=30.3$ kcal mol^{-1}). In another earlier study[13] we compared the reaction mechanisms of the [2+2+2] cycloaddition reaction of three acetylene molecules catalysed by $[RhCl(PPh_3)_3]$ and $[RhCl(PH_3)_3]$. The main difference we found in the Gibbs energy profiles for the two catalysts is the initial phosphine dissociation step,[17] which is very favoured with the $[RhCl(PPh_3)_3]$ catalyst.[13,14,17] This result is not unexpect-

 © 2011 Wiley-VCH Verlag GmbH & Co. KGaA, Weinheim

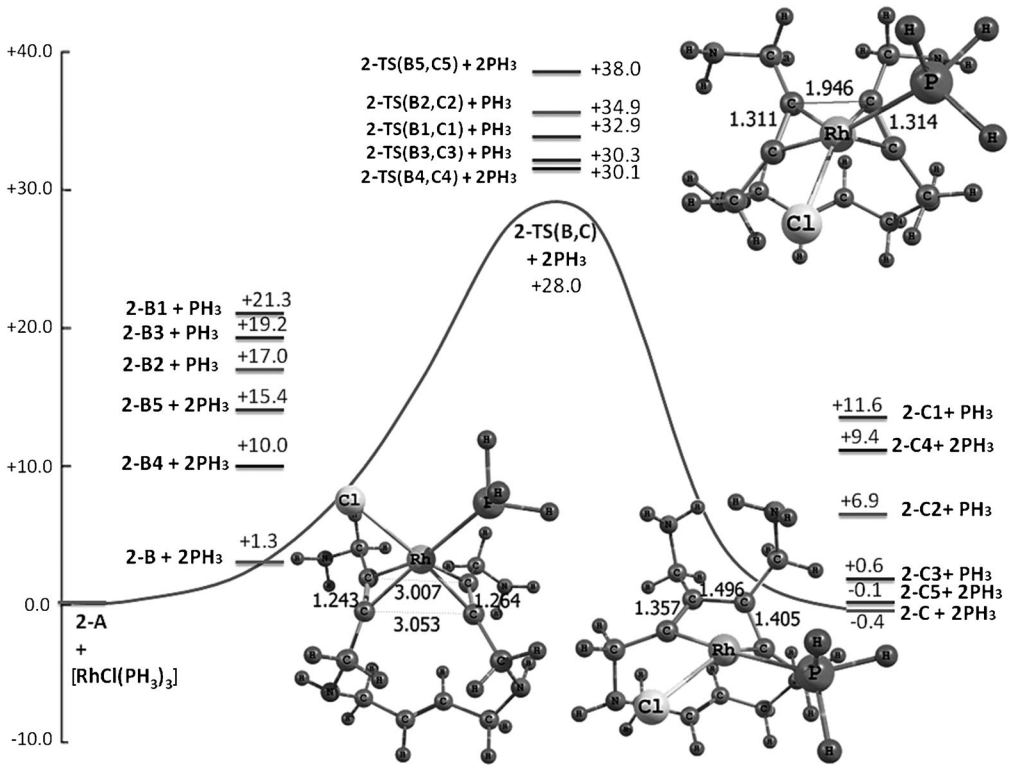

Figure 4. Gibbs energy profiles for the different oxidative coupling steps: Enyne couplings via **2-TS(B1,C1)** and **2-TS(B2,C2)** when the rhodium catalyst has two attached phosphine ligands, and via **2-TS(B4,C4)** and **2-TS(B5,C5)** when it has only one PH_3 ligand attached. Alkyne–alkyne coupling via **2-TS(B3,C3)** when the rhodium catalyst has two phosphine ligands and via **2-TS(B,C)** when it has only one phosphine attached. Energies in kcal mol^{-1} and distances in Å

ed given the different electronic and steric effects exerted by the PPh_3 ligands as compared with PH_3. Our previous study[13] led us to expect that the Gibbs energy profiles for the [2+2+2] cycloaddition reactions of the enediynes studied would be slightly lower if computed with the $[RhCl(PPh_3)_3]$ catalyst.[13,14,17]

If we study the 16-electron **2-C** complex (arising from alkyne–alkyne oxidative addition with $[RhCl(PH_3)]$), two possibilities emerge from this point (Figures 5 and 6). First, a phosphine ligand can be attached to complex **2-C** to yield **2-C3**. This process is endoergonic by 1.2 kcal mol^{-1}. Secondly, intramolecular coordination of the alkene moiety to yield complex **2-D** can take place with an energy stabilisation of 26.6 kcal mol^{-1}. Therefore, coordination of the alkene is more favoured than the attachment of an incoming PH_3 ligand. The olefin is then inserted with an energy barrier of $\Delta G^{\neq} = 15.5$ kcal mol^{-1} to give the rhodacycloheptadiene intermediate **2-E** via **2-TS(D,E)**, leaving only one face to be coordinated due to system constraints.

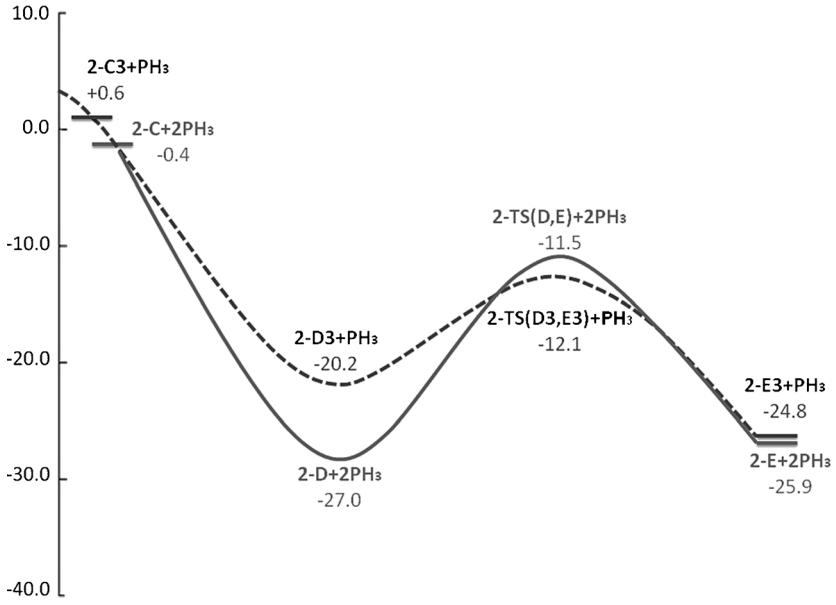

Figure 5. Gibbs energy profiles (in kcal mol^{-1}) for the two possible insertions of an alkene moiety: From **2-D** to form complex **2-E** via the transition state **2-TS(D,E)** and from complex **2-D3** to form **2-E3** via **2-TS(D3,E3)** for enediyne model **2-A**.

 © 2011 Wiley-VCH Verlag GmbH & Co. KGaA, Weinheim

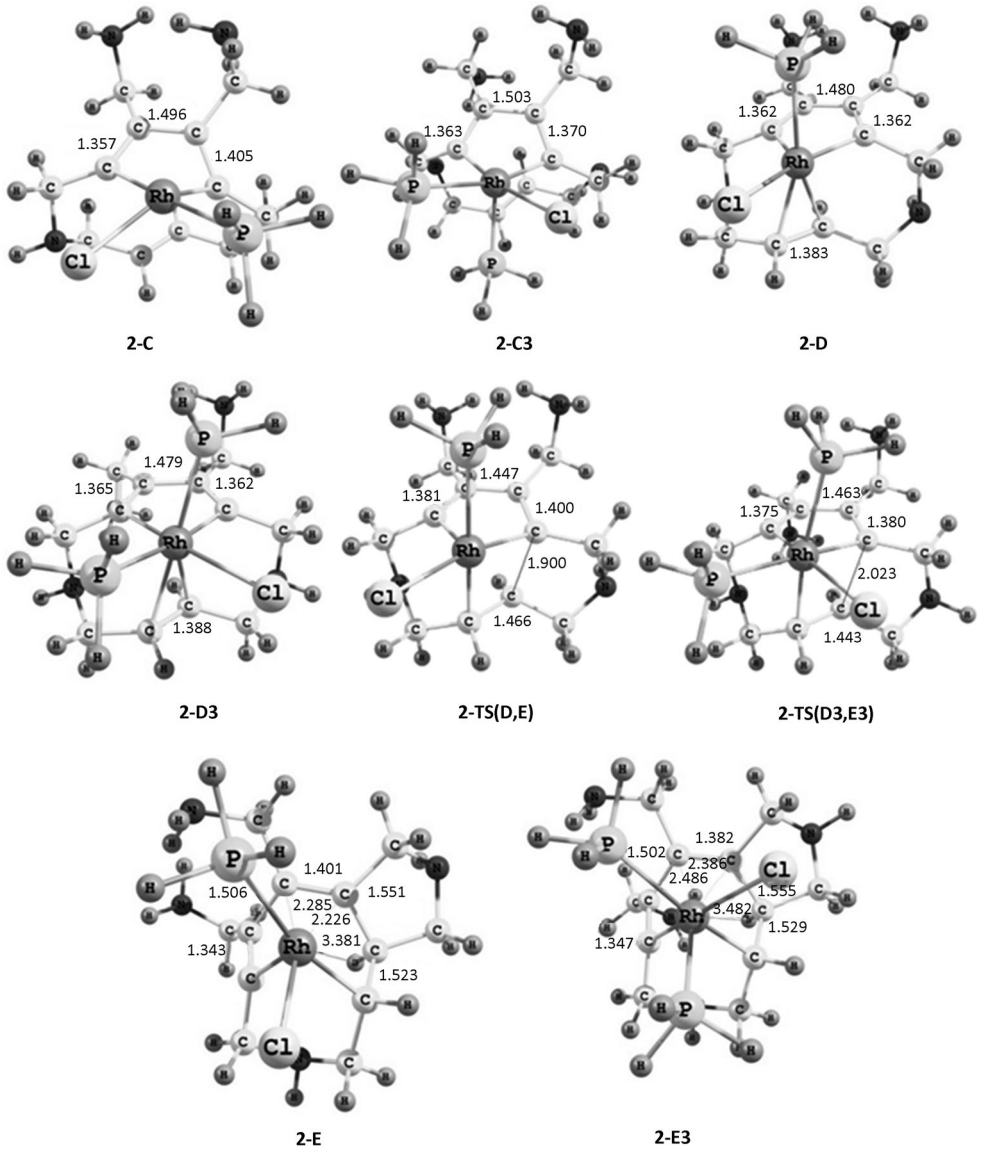

Figure 6. Structures of the reactants, intermediates, transition states and products optimised at the B3LYP level of theory for the transformation of **2-C** to **2-E** and of **2-C3** to **2-E3** with selected bond distances [Å].

On the other hand, if we study the 18-electron complex **2-C3** (arising from alkyne–alkyne oxidative addition and $[RhCl(PH_3)_2]$; Figures 5 and 6), the coordination of the alkene moiety to yield complex **2-D3** releases 20.8 kcal mol^{-1}. The olefin is then inserted into complex **2-D3** to afford the rhodacycloheptadiene complex **2-E3** via **2-TS-(D3,E3)** with a barrier of $\Delta G^{\neq} = 8.1$ kcal mol^{-1}. With these results we observe that the two reaction pathways have slightly different energy requirements but that they could both be operative.

Continuing the DFT calculations from the complexes **2-E** and **2-E3**, the next step is ring closure (Figure 7). At this point we observe that **2-E** and **2-E3** have no hydrogen atoms at the β position that can be eliminated (the closest H_β is at 3.38 and 3.48 Å, respectively, from the rhodium; Figure 6). For this reason, β-hydride elimination could not take place in this case. Starting from complex **2-E3**, ring closure takes place via **2-TS(E3,F3)** with a Gibbs energy barrier of 24.9 kcal mol^{-1} (Figure 7), although it is an exoergonic step ($\Delta G° = -12.1$ kcal mol^{-1}). This process yields complex **2-F3** in which the rhodium atom is coordinated through a three-centre–four-electron (3c–4e) intramolecular metal–hydrogen bond (IMHB) to the H_α atom of the cyclohexadiene ring formed (the values of Rh–H_α 1.86 Å, Rh–C 2.88 Å and $\measuredangle CH_\alpha Rh$ 143.5° rule out the possibility of an agostic interaction and are typical of IMHBs[18]). Finally, the catalytic cycle is closed upon exoergonic displacement (by 27.3 kcal mol^{-1}) of the cyclohexadiene product **2-H** by a phosphine molecule to regenerate the $[RhCl(PH_3)_3]$ catalyst (Figure 7).

When the reaction mechanism evolves from intermediate **2-E** via **2-TS(E,F)** ($\Delta G^{\neq} = 13.1$ kcal mol^{-1}) a fused tricyclic complex **2-F**, in which the arene ring is coordinated in an η^4

 © 2011 Wiley-VCH Verlag GmbH & Co. KGaA, Weinheim

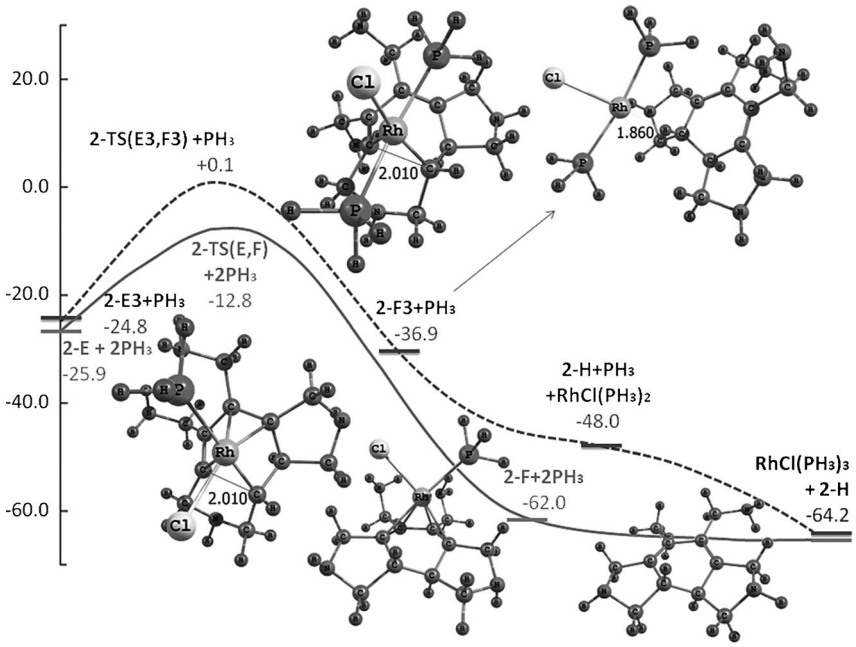

Figure 7. Gibbs energy profiles (in kcal mol^{-1}) for the formation of the product **2-H** from **2-E** and **2-E3**.

fashion, is obtained. Complex **2-F** then evolves to the cyclohexadiene product (**2-H**) by adding two phosphine molecules to regenerate the [RhCl(PH$_3$)$_3$] catalyst. Note that intermediates **2-F** and **2-F3** are different complexes although both transition states correspond to ring closure. Therefore the pathway followed depends on the number of PH$_3$ ligands attached to the rhodium atom.

The complete reaction mechanism for the rhodium-catalysed reaction of enediynes **1** and **2** deriving from our analysis is presented in Figure 8. There are two main pathways that yield **2-H** from **2-A** that differ in the active catalyst: [RhCl(PH$_3$)$_2$] (dashed line) and [RhCl(PH$_3$)] (solid line). Our results show that both pathways may be operative given the similar energy requirements.

*Yne-yne-ene enediynes **3** and **4***: We then examined the reaction mechanism for enediynes **3** and **4**, which did not afford the standard [2+2+2] cycloadducts. These two compounds only differ in the protecting group (Boc) in the terminal amine connected to the alkene. We studied a model of these enediynes with primary amines (model **4-A** in Scheme 4). The Boc group does not seem to have a significant influence on the reaction mechanism as the two enediynes **3** and **4** behave similarly in the presence of the Wilkinson catalyst.

As for model **2-A**, we analysed the different possibilities for the oxidative coupling step in model **4-A** (Scheme 4). Thus, as can be seen in Figure 9, the Wilkinson catalyst can interact with the two adjacent triple bonds or with the double bond and the consecutive triple bond of the enediyne. In addition, we have taken into account the fact that both [RhCl(PH$_3$)$_2$] and [RhCl(PH$_3$)] may be the active species of the catalyst, as we have seen previously.

When the catalytic species is [RhCl(PH$_3$)$_2$], the most favourable of the three C–C oxidative coupling reactions is the alkyne–alkyne coupling that transforms **4-B** into **4-C** via **4-TS(B,C)** with the lowest barrier of $\Delta G^{\neq} = 22.1$ kcal mol^{-1}. In this process the [RhCl(PH$_3$)$_3$] catalyst first loses a PH$_3$ ligand and then interacts with **4-A** to yield a distorted trigonal-bipyramidal complex **4-B** by replacing one phosphine with two internal η^2 interactions with adjacent acetylenic units of **4-A**. Note that the transformation of **4-A** into **4-B** is endoergonic by 16.7 kcal mol^{-1}, although this endoergonicity

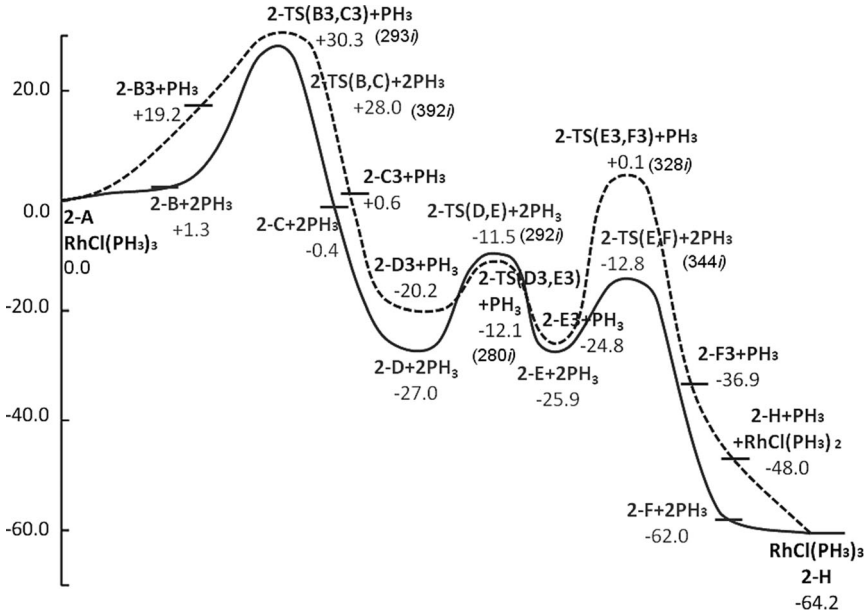

Figure 8. Gibbs energy profiles for the [2+2+2] cycloaddition of model **2-A** (enediynes **1** and **2**) in which the active catalyst is [RhCl(PH$_3$)$_2$] (dashed line) or [RhCl(PH$_3$)] (solid line). Relative Gibbs energies with respect to separated reactants in kcal mol^{-1}. Imaginary frequencies [cm^{-1}] for the different transition states are given in brackets.

 © 2011 Wiley-VCH Verlag GmbH & Co. KGaA, Weinheim

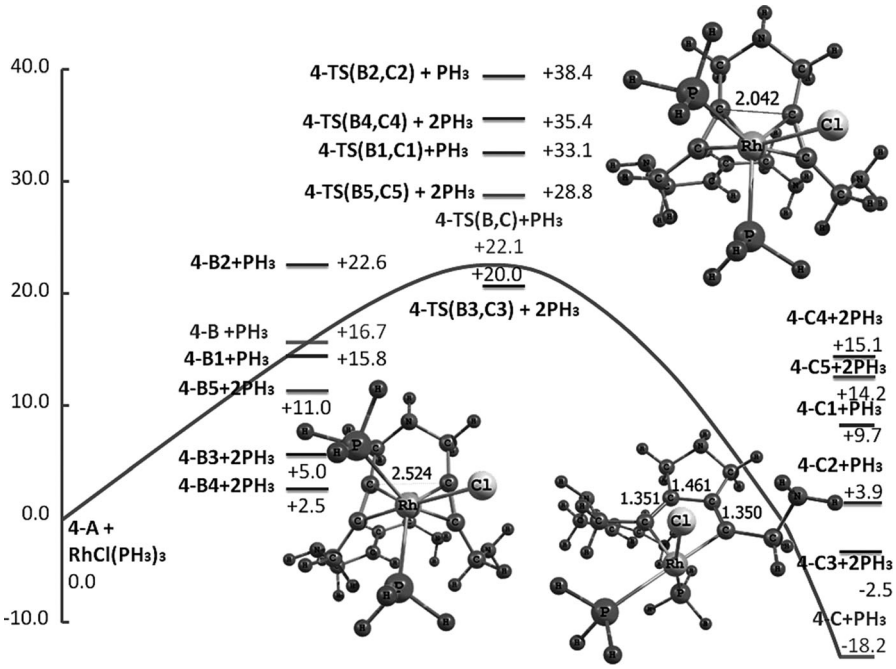

Figure 9. Gibbs energy profiles (in kcal mol^{-1}) for the different oxidative coupling steps: Enyne couplings via **4-TS(B1,C1)** and **4-TS(B2,C2)** when the rhodium has two phosphine ligands attached and via **4-TS(B4,C4)** and **4-TS(B5,C5)** when there is only one PH_3 ligand attached, and alkyne–alkyne couplings via **4-TS(B,C)** when the rhodium has two phosphine ligands and via **4-TS(B3,C3)** when the rhodium has only one phosphine attached. Energies in kcal mol^{-1} and distances in Å.

is probably overestimated as a result of substitution of the PPh_3 ligands in the Wilkinson catalyst by a stronger σ donor, such as PH_3.[17] The other two possible oxidative addition reactions correspond to the coordination of the alkene and alkyne moieties (**4-B1** and **4-B2**) to yield the distorted rhodacyclopentene adducts **4-C1** and **4-C2** via **4-TS(B1,C1)** ($\Delta G^{\neq}=33.1$ kcal mol^{-1}) and **4-TS(B2,C2)** ($\Delta G^{\neq}=38.4$ kcal mol^{-1}), respectively.

On the other hand, when the rhodium retains only one PH_3 ligand, that is, the catalytic species is [RhCl(PH_3)], the alkyne–alkyne coupling reaction transforming **4-B3** into **4-C3** via **4-TS(B3,C3)** with $\Delta G^{\neq}=20.0$ kcal mol^{-1} is clearly the most favourable oxidative coupling. The enyne couplings of complexes **4-B4** and **4-B5** leading to the rhodacyclopentene adducts **4-C4** and **4-C5** via **4-TS(B4,C4)** ($\Delta G^{\neq}=35.4$ kcal mol^{-1}) and **4-TS(B5,C5)** ($\Delta G^{\neq}=28.8$ kcal mol^{-1}), respectively, have energy barriers that are higher by about 10–15 kcal mol^{-1}.

There is a clear preference for the alkyne–alkyne coupling over the enyne coupling reactions irrespective of whether the [RhCl(PH_3)$_2$] or [RhCl(PH_3)] catalytic species is used, in agreement with a previous study showing that alkyne–alkyne coupling is usually preferred.[16] Our results therefore show that the pathway following the enyne coupling can be ruled out and for this reason we continued our study from species **4-C**, which is the most stable species resulting from the different oxidative couplings analysed. Although species **4-C3** is kinetically favoured (although not thermodynamically) over **4-C**, we have decided only to follow the analysis from species **4-C** given that our previous study of model **2-A** revealed that the reaction mechanism is similar in both cases.

The oxidative coupling of the two alkynes **4-B**→**4-C** leads to the distorted trigonal-bipyramidal rhodacyclopentadiene **4-C** with a Gibbs stabilisation energy of 34.9 kcal mol^{-1}. In the next step, the formation of two stereoisomers (**4-D** and **4-D1**) is possible through the coordination of the two faces of the olefin, which now have no steric constraints. Moreover, the olefin can be inserted into each one of the two nonequivalent Rh–C bonds of the rhodacyclopentadiene. For this reason, the energies of the alkene–rhodacyclopentadiene stereoisomers **4-D** and **4-D1** were computed with the corresponding TSs of the C–C coupling reactions leading to the fused bicyclic ring systems **4-E**, **4-E1**, **4-E2** and **4-E3** (Scheme 5). The [4+2] cycloaddition reaction was also investigated, but all attempts were unsuccessful and no TS for this route was located. We therefore discarded this possible pathway and focused on the pathways shown in Scheme 5.

The rhodacyclopentadiene complexes **4-D** and **4-D1** have similar stabilities with respect to the reactants. Of the different activation processes, the one with the greatest cost in terms of energy is the transformation of **4-D1** into **4-E2** via **4-TS(D1,E2)** ($\Delta G^{\neq}=21.2$ kcal mol^{-1}) followed by the transformation of **4-D1** into **4-E3** via **4-TS(D1,E3)** ($\Delta G^{\neq}=16.5$ kcal mol^{-1}). We were unable to locate the TS corresponding to the transformation of **4-D** into **4-E1** and all our attempts led to the TS for the transformation of **4-D** into **4-E**, which has the lowest energy barrier of $\Delta G^{\neq}=8.1$ kcal mol^{-1}. Therefore, we concluded that the preferred pathway is the C–C coupling reaction between the alkene moiety coordinated to the rhodacyclopentadiene **4-D** via **4-TS(D,E)**, which leads to the rhodabicyclic ring system **4-E**.

There are two different pathways from complex **4-E** (Figure 10). The first is a C–C bond formation and a Rh–C bond cleavage assisted by an H_β agostic interaction via the transition state **4-TS(E,F)** with $\Delta G^{\neq}=14.5$ kcal mol^{-1}. This process leads to **4-F** in which the rhodium atom has a distorted octahedral geometry and maintains an agostic interaction with H_β (the values of Rh–H_β 1.88 Å, Rh–C 2.31 Å and $\measuredangle CH_\beta Rh$ 95.2° are typical of agostic interactions[18]). This H_β agostic interaction is similar to that found for the ruthenium system of Saá and co-workers,[8b] which has similar distances (Ru–H_β 1.82 Å, Ru–C 2.40 Å and $\measuredangle CH_\beta Ru$

 © 2011 Wiley-VCH Verlag GmbH & Co. KGaA, Weinheim

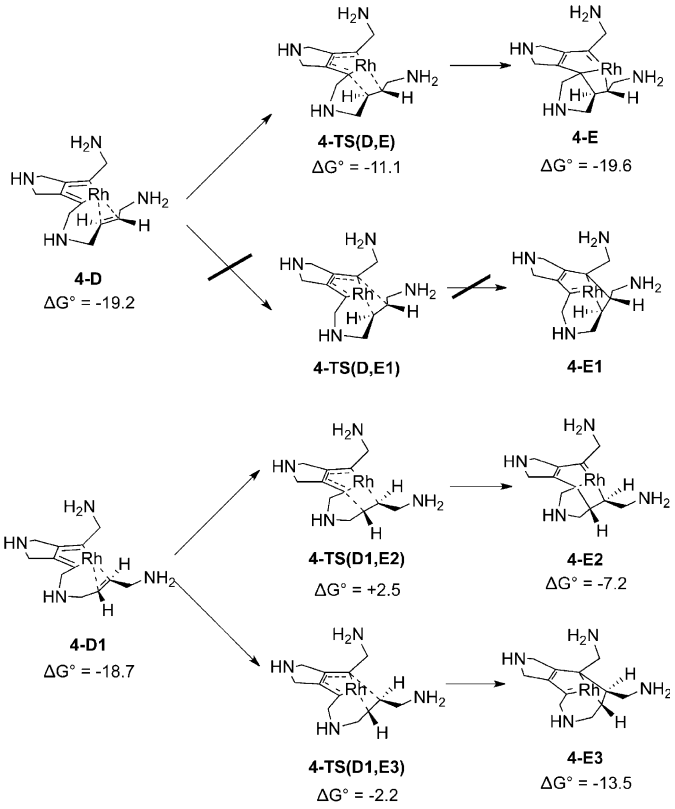

Scheme 5. Possible stereoisomers resulting from the coordination of the rhodacyclopentadiene complex to the double bond of the open chain and possible C–C couplings in each case. Gibbs energy values given relative to **4-A** are in kcal mol^{-1}.

103.1°) but a higher energy barrier for the transformation ($\Delta G^{\neq}=21.8$ kcal mol^{-1}). The second pathway is an electrocyclic opening of the complex **4-E** to give the rhodacycloheptadiene **4-F1**. The barrier of **4-TS(E,F1)** ($\Delta G^{\neq}=7.2$ kcal mol^{-1}) is lower than that of **4-TS(E,F)**, in line with the results reported by Saá and co-workers, for which this pathway was also found to have the lower Gibbs energy ($\Delta G^{\neq}=12.2$ kcal mol^{-1}).[8b]

Therefore, we followed the reaction pathway from both intermediates **4-F** and **4-F1** (Figures 11 and 12). From **4-F1** the ring can be closed via **4-TS(F1,I2)**, which has a high barrier of 24.5 kcal mol^{-1}, to give the 3c–4e IMHB intermediate **4-I2** (dashed line in Figure 11). This transformation has a high energy barrier and, taking into account the fact that **4-TS(E,F1)** has a low barrier, the process that connects **4-E** with **4-F1** may be reversible and may follow the alternative reaction pathway (**4-F1**→**4-E**→**4-F**→**4-G**→**4-H**), which has lower-energy requirements.

From **4-F**, we found two different pathways (Figures 11 and 12). First, path A (dotted line, **4-F**→**4-J1**) involves reductive elimination, leading to the cyclohexadiene product after ring slippage and regeneration of the Wilkinson catalyst (see the optimised intermediates in Figure 12). The TS ($\Delta G^{\neq}=7.0$ kcal mol^{-1}) of this process (**4-TS(F,I1)**) requires the loss of one phosphine ligand, leading to a fused tricyclic complex **4-I1** in which the arene ring is coordinated in an η^4 fashion to the metal (see Figure 12). This intermediate then evolves to the cyclohexadiene product **4-J1** adding two phosphine molecules to regenerate the [RhCl(PH$_3$)$_3$] catalyst. This compound, **4-J1**, is the expected product of the [2+2+2] cycloaddition (**12** and **13** in Scheme 3) but not the experimentally obtained product (**14** and **15** in Scheme 3). Secondly, path B (solid line in Figure 11) entails a β-hydride elimination from **4-F** via **4-TS(F,G)** ($\Delta G^{\neq}=5.8$ kcal mol^{-1}) to afford the complex **4-G** as a rhodium hydride distorted octahedral complex in which the rhodium is coordinated in an η^3 fashion to the six-membered ring (see Figure 12). Next, the release of one PH$_3$ ligand is required to give the tetra-coordinated complex **4-H** (stabilised by 22.8 kcal mol^{-1} with respect to **4-G**). Although we have not located the TS corresponding to the **4-G**→**4-H** process, we expect a small barrier for this exergonic loss of a phosphine ligand. The intermediate **4-H** has an adequate conformation for reductive elimination via **4-TS(H,I)** ($\Delta G^{\neq}=11.5$ kcal mol^{-1}), leading to the fused tricyclic complex **4-I** in which the rhodium is coordinated in an η^2 fashion to the arene ring and the metal also has an agostic interaction with H_β (Rh–H_β 1.79 Å, Rh–C

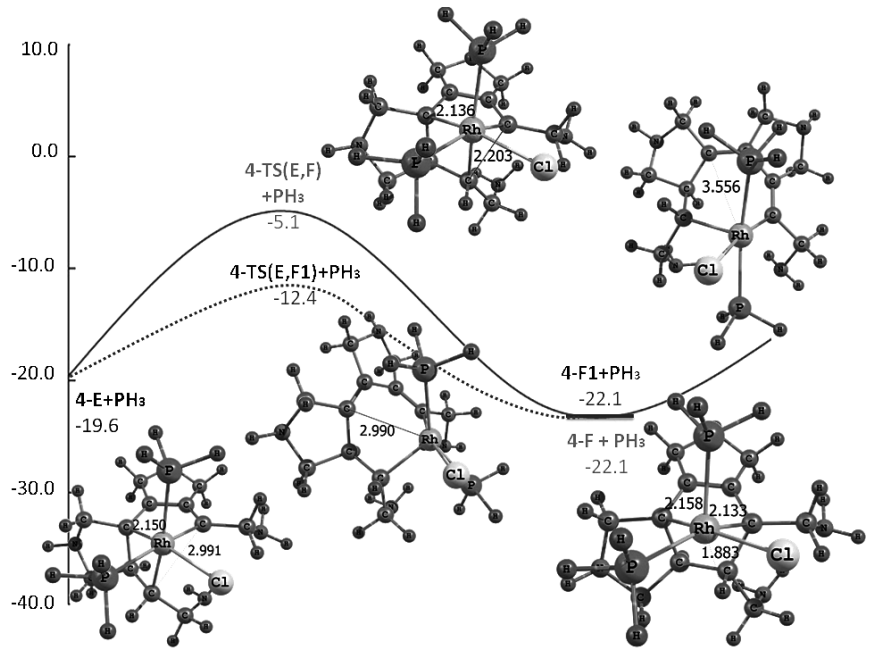

Figure 10. Gibbs energy profiles (in kcal mol^{-1}) for the formation of complexes **4-F** and **4-F1** via the transition states **4-TS(E,F)** and **4-TS(E,F1)**, respectively, with selected bond distances [Å].

 © 2011 Wiley-VCH Verlag GmbH & Co. KGaA, Weinheim

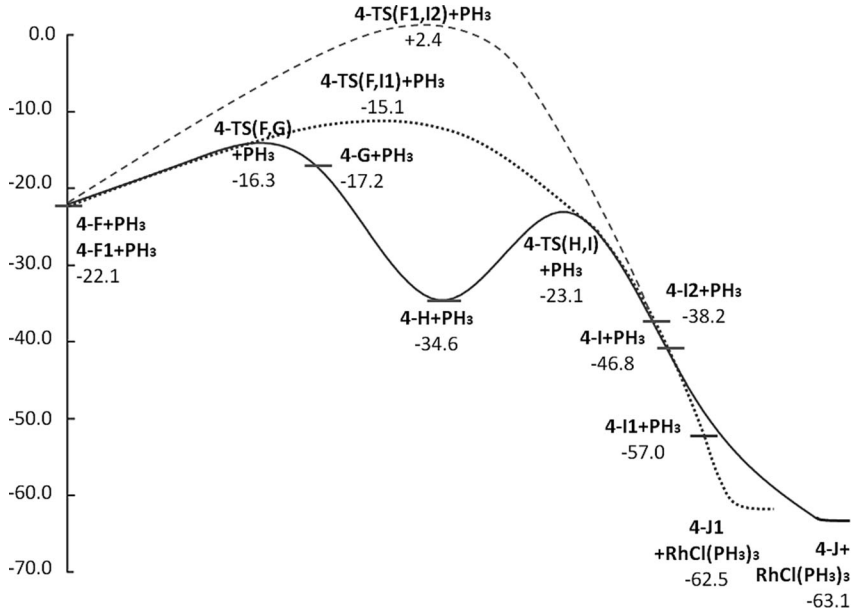

Figure 11. Gibbs energy profiles (in kcal mol^{-1}) for the formation of **4-J** which is the model for products **14** and **15**.

2.38 Å and $\measuredangle CH_\beta Rh$ 103.2°). The displacement of the arene **4-J** and the regeneration of the $[RhCl(PH_3)_3]$ catalyst is the next conversion. This compound, **4-J**, coincides with the product obtained experimentally (**14** and **15** in Scheme 3; see the optimised intermediates in Figure 12), which is thermodynamically 0.6 kcal mol^{-1} more stable than the expected product (**4-J1**). Therefore, path B accounts for the rhodium-catalysed reactions of enediynes **3** and **4** affording the final experimental product observed. Both thermodynamically and kinetically, **4-J** is slightly favoured over **4-J1** by a few kcal mol^{-1}. We also analysed the process that does not stop at the rhodium hydride **4-H**, in which H_β is transferred directly to the α carbon to give complex **4-I3** (direct transformation **4-F-4-I3** is not shown in Figure 11). Given that the energy barrier of this process is too high (**4-TS(F,I3)**, $\Delta G^{\neq} =$ 30.7 kcal mol^{-1}) for it to take place instead of the **4-F**→**4-G**→**4-H**→**4-I** pathway, we discarded the possibility of this direct transformation being operative.

The energy profile for the whole mechanism of the reactions of the enediynes **3** and **4** catalysed by $[RhCl(PH_3)_3]$ is presented in Figure 13 whereas Scheme 6 provides a summary of the catalytic cycle proposed for the [2+2+2] cycloaddition reactions of enediynes **3** and **4**. There are several differences between the present β-elimination mechanism and that found for Cp*Ru (Cp* = 1,2,3,4,5-pentamethylcyclopentadienyl) and CpCo systems. First, we did not observe metallacycloheptadiene but rather bicyclic intermediates. Secondly, our final product is the cyclohexadiene product, whereas for the other systems the final product is a 1,3,5-hexatriene species. Finally, it is pertinent to point out that a recent B3LYP/LANL2DZ-6-31G* study[19] has shown that a similar β-hydride elimination can compete with the [3+2] pathway in the Rh^{I}-catalysed intramolecular [3+2] cycloaddition reactions of 1-ene-vinylcyclopropanes. Similar to our proposed mechanism, this β-hydride elimination also involves an intermediate with a Rh–H bond.

Conclusion

The paths of the rhodium-catalysed intramolecular [2+2+2] cycloaddition reactions of enediynes **1**–**4** to give the corresponding cyclohexadienes vary with the position of the alkene moiety in the enediyne. For enediyne model **2-A** (yne-ene-yne), the standard [2+2+2] cycloaddition reaction giving compounds **10** and **11** is preferred as the key intermediates **2-E** and **2-E3** cannot undergo β-hydride elimination due to the large distance between the rhodium and H_β atoms. In contrast, the enediyne model **4-A** (yne-yne-ene) undergoes β-hydride elimination followed by reductive elimination of the Wilkinson catalyst to yield cycloadducts **14** and **15**, which are isomers of the products that would be obtained by standard [2+2+2] cycloaddition reactions. In this case, the key intermediate is the complex **4-F** in which an agostic interaction between rhodium and hydrogen allows β-hydride elimination. Experimental observations and DFT calculations support the mechanism proposed.

Experimental Section

Unless otherwise noted, materials were obtained from commercial suppliers and used without further purification. All reactions requiring anhydrous conditions were conducted in oven-dried glassware under a dry nitrogen atmosphere. All solvents were distilled over appropriate drying reagents (sodium or calcium hydride) in an inert atmosphere. The solvents were removed under reduced pressure with a rotary evaporator. Residues were purified by chromatography on a silica gel column (230–400 mesh) by using a gradient solvent system (hexane/ethyl acetate or hexane/dichloromethane) as the eluent.

^{1}H and ^{13}C NMR spectra were measured on a 600 or a 200 MHz NMR spectrometer. ^{1}H and ^{13}C chemical shifts (δ) are referenced to internal solvent resonances and reported relative to $SiMe_4$. The chemical shifts were assigned on the basis of 2D COSY, NOESY, HSQC and HMBC experiments performed under routine conditions.

N-(4-Bromo-2-butynyl)-*N*-(*tert*-butyloxycarbonyl)-4-methylphenylsulfonamide (**5**), 1,11-bis(*tert*-butyloxycarbonyl)-1,6,11-tris(4-methylphenylsulfonyl)-1,6,11-triazaundeca-3,8-diyne (**7**) and 1,6,11-tris(4-methylphenylsulfonyl)-1,6,11-triazaundeca-3,8-diyne (**8**) were prepared as previously reported by our group.[12a] (*E*)-*N*,*N*′-Bis(4-methylphenylsulfonyl)-2-butene-1,4-diamine (**6**)[12b] and *N*-[(*E*)-4-bromo-2-butenyl]-*N*-(*tert*-butyloxycarbonyl)-4-methylphenylsulfonamide (**9**)[12b] were prepared as previously reported.

 © 2011 Wiley-VCH Verlag GmbH & Co. KGaA, Weinheim

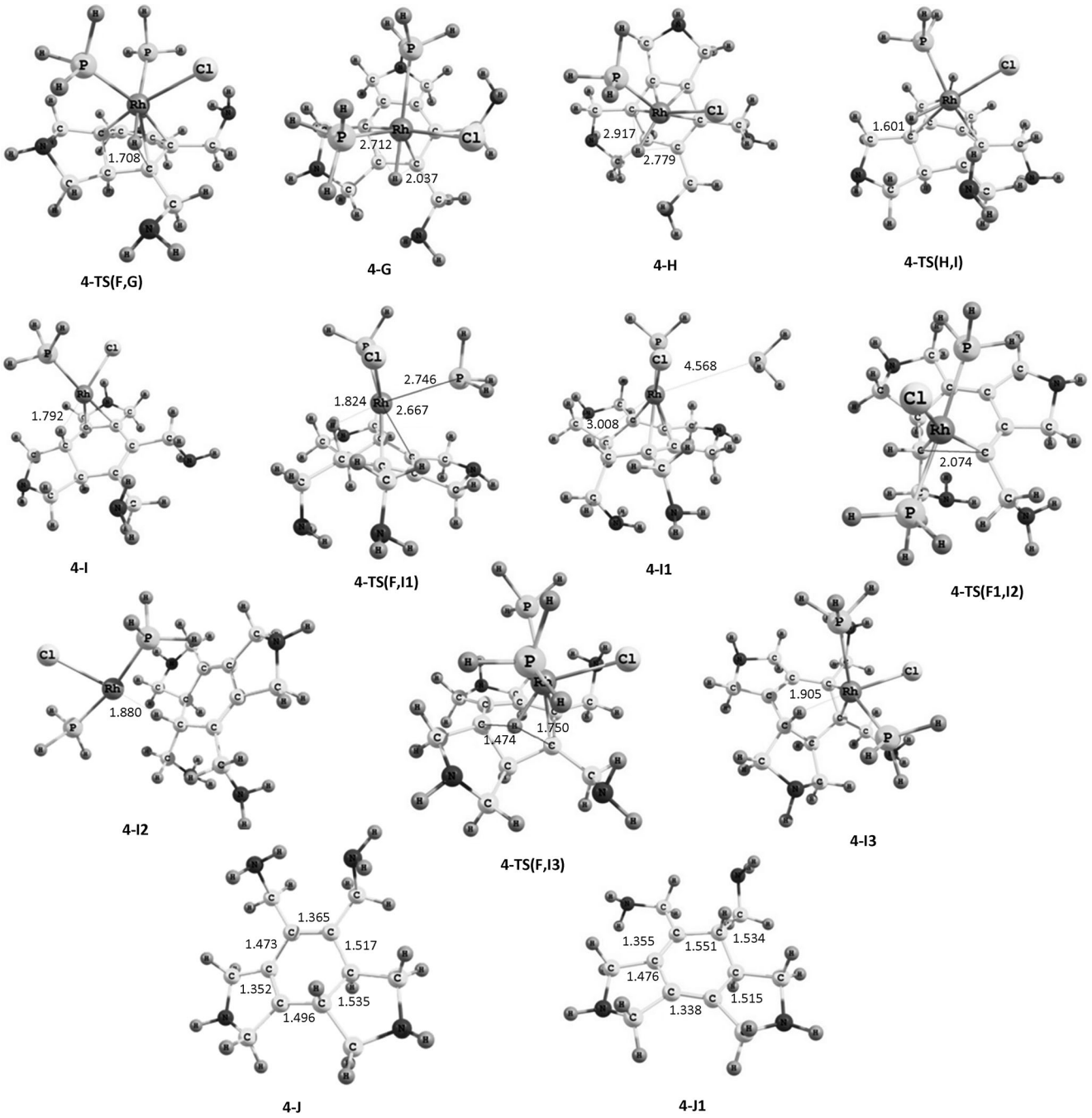

Figure 12. Structures of the intermediates optimised at the B3LYP level of theory for the transformation of **4-F1** into **4-I2** and the intermediates of paths A and B with selected bond distances [Å].

1,16-Bis((*tert*-butyloxycarbonyl)-1,6,11,16-tetrakis(4-methylphenylsulfonyl)-1,6,11,16-tetraazahexadeca-8-ene-3,13-diyne (1): A stirred mixture of **6** (0.60 g, 1.52 mmol), potassium carbonate (1.08 g, 7.61 mmol) and acetonitrile (40 mL) was heated at reflux for 10 min. Then a solution of *N*-(4-bromo-2-butynyl)-*N*-(*tert*-butyloxycarbonyl)-4-methylphenylsulfonamide (**5**; 1.23 g, 3.05 mmol) in acetonitrile (10 mL) was added slowly to the reaction mixture. The reaction was heated and monitored by TLC until completion (20 h). The salts were filtered off and the filtrate was evaporated. The residue was purified by column chromatography on silica gel with hexanes/ethyl acetate (polarity from 8:2 to 6:4) to afford **1** (1.20 g, 75%) as a colourless solid. M.p. 78–80°C; ^{1}H NMR (200 MHz, $CDCl_3$, 25°C, TMS): $\delta = 1.32$ (s, 18H), 2.42 (s, 6H), 2.44 (s, 6H), 3.70–3.79 (m, 4H), 4.05 (br s, 4H), 4.39 (br s, 4H), 5.55–5.61 (m, 2H), 7.27–7.35 (m, 8H), 7.71 (AA′BB′ system, ^3J(H,H) = 8.2 Hz, 4H), 7.81 ppm (AA′BB′ system, ^3J(H,H) = 8.4 Hz, 4H); ^{13}C NMR (50 MHz, $CDCl_3$, 25°C, TMS): $\delta = 22.2$, 22.3, 28.5, 36.2, 37.0, 48.5, 77.4, 81.8, 85.7, 128.3, 128.6, 129.7, 130.1, 130.4, 136.6, 137.4, 144.5, 145.3, 150.8 ppm; IR (ATR): $\tilde{\nu} = 2981$, 1735, 1344, 1159 cm^{-1}; HRMS (ESI): *m*/*z* calcd for $C_{50}H_{60}N_4S_4O_{12}$+Na^+: 1059.2983; found: 1059.2947.

1,6,11,16-Tetrakis(4-methylphenylsulfonyl)-1,6,11,16-tetraazahexadeca-8-ene-3,13-diyne (2): A mixture of **1** (0.80 g, 0.78 mmol), trifluoroacetic acid (3.2 mL) and dichloromethane (10 mL) was stirred at room tempera-

 © 2011 Wiley-VCH Verlag GmbH & Co. KGaA, Weinheim

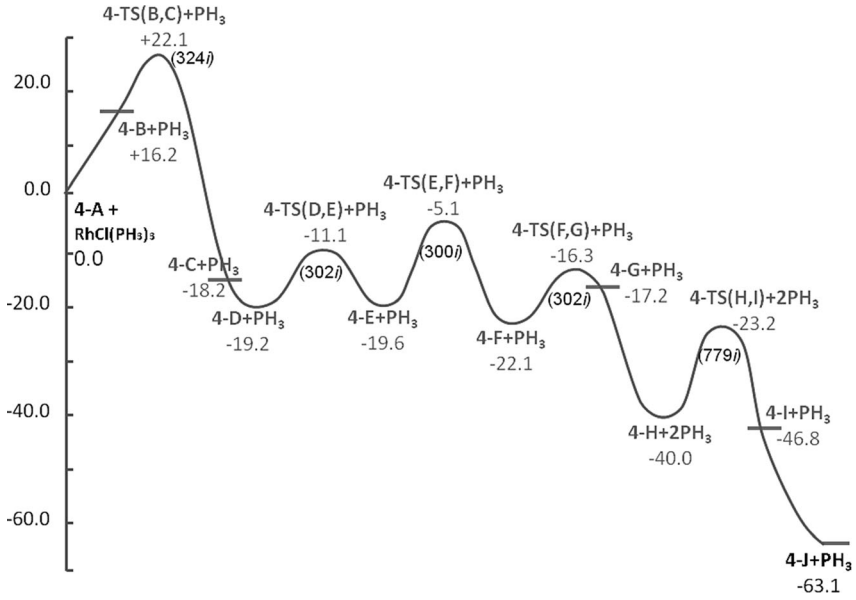

Figure 13. Gibbs energy profile for the [2+2+2] cycloaddition of the model of enediynes **3** and **4**. Gibbs energy values relative to the initial reactants are in kcal mol^{-1}. Imaginary frequencies [cm^{-1}] for the different transition states are given in parentheses.

ture for 7 h (TLC monitoring). The liquid was distilled off under vacuum and the residue was dissolved in ethyl acetate (20 mL). The organic layer was subsequently washed with aqueous sodium bicarbonate (3×20 mL), H_2O (3×20 mL) and brine (20 mL), dried (Na_2SO_4) and filtered. The solvent was evaporated under reduced pressure to afford **2** (0.60 g, 98%) as a colourless solid. M.p. 85–88°C; ^{1}H NMR (200 MHz, $CDCl_3$, 25°C, TMS): δ=2.42 (s, 6H), 2.44 (s, 6H), 3.52 (t, ^3J(H,H)=1.8 Hz, 2H), 3.55 (t, ^3J(H,H)=2 Hz, 2H), 3.60–3.69 (m, 4H), 3.87 (br s, 4H), 4.68 (t, ^3J(H,H)=5.9 Hz, 2H), 5.50–5.61 (m, 2H), 7.27–7.35 (m, 8H), 7.66 (AA′BB′ system, ^3J(H,H)=8.2 Hz, 4H), 7.71 ppm (AA′BB′ system, ^3J(H,H)=8.4 Hz, 4H); ^{13}C NMR (50 MHz, $CDCl_3$, 25°C, TMS): δ=22.2, 33.4, 37.2, 48.8, 78.2, 80.9, 127.9, 128.4, 129.8, 130.3, 130.4, 136.4, 137.2, 144.5, 144.7 ppm; IR (ATR): $\tilde{\nu}$=3249, 2923, 1331, 1155 cm^{-1}; HRMS (ESI): *m*/*z* calcd for $C_{40}H_{44}N_4S_4O_8$+Na$^+$: 859.1934; found: 859.1893.

1,16-Bis(*tert*-butyloxycarbonyl)-1,6,11,16-tetrakis(4-methylphenylsulfonyl)-1,6,11,16-tetraazahexadeca-3-ene-8,13-diyne (3): A stirred mixture of **8** (0.92 g, 1.50 mmol), potassium carbonate (0.53 , 3.75 mmol) and acetonitrile (100 mL) was heated at reflux for 10 min. Then a solution of *N*-[(*E*)-4-bromo-2-butenyl]-*N*-(*tert*-butyloxycarbonyl)-4-methylphenylsulfonamide (**9**; 0.30 g, 0.75 mmol) in acetonitrile (10 mL) was added slowly to the reaction mixture. The reaction was heated and monitored by TLC until completion (4 h). The salts were filtered off and the filtrate was evaporated. The residue was purified by column chromatography on silica gel with dichloromethane/ethyl acetate (polarity 40:1) to afford **3** (0.50 g, 75%) as a colourless solid. M.p. 76–80°C; ^{1}H NMR (200 MHz, $CDCl_3$, 25°C, TMS): δ=1.32 (s, 9H), 2.44 (m, 12H), 3.58 (d, ^3J(H,H)=6 Hz, 2H), 3.70 (d, ^3J(H,H)=6 Hz, 2H), 3.79 (m, 4H), 3.95 (br s, 2H), 4.36 (d, ^3J(H,H)=6 Hz, 2H), 4.73 (t, ^3J(H,H)=6 Hz, 1H), 5.70 (m, 2H), 7.32 (m, 8H), 7.60 (AA′BB′ system, ^3J(H,H)=8.4 Hz, 2H), 7.68 (AA′BB′ system, ^3J(H,H)=8.4 Hz, 2H), 7.69 (AA′BB′ system, ^3J(H,H)=8.4 Hz, 2H), 7.74 ppm (AA′BB′ system, ^3J(H,H)=8.4 Hz, 2H); ^{13}C NMR (50 MHz, $CDCl_3$, 25°C, TMS): δ=20.7, 20.8, 27.1, 32.1, 35.5, 35.6, 46.9, 47.1, 76.1, 77.4, 77.9, 79.5, 83.9, 126.5, 126.8, 126.9, 127.0, 127.1, 128.6, 128.8, 128.9, 130.2, 134.3, 134.9, 135.9, 136.3, 143.0, 143.2, 143.5, 143.7, 149.9 ppm; IR (ATR): $\tilde{\nu}$=3275, 2974, 1725, 1345, 1155 cm^{-1}; HRMS (ESI): *m*/*z* calcd for $C_{45}H_{52}N_4S_4O_{10}$+Na$^+$: 959.2458; found: 959.2414.

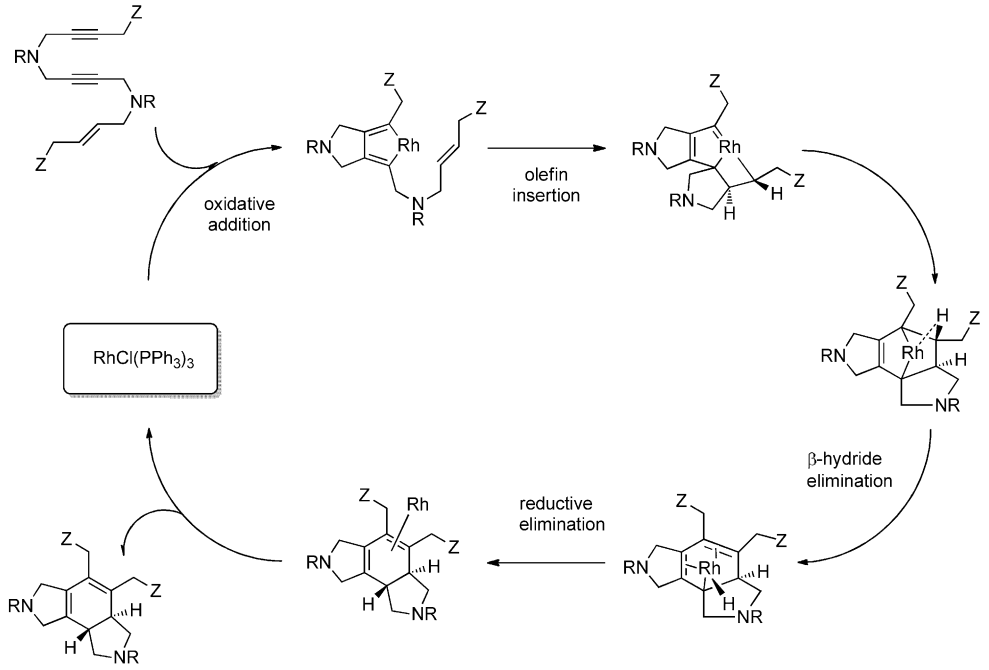

Scheme 6. Catalytic cycle proposed for the intramolecular [2+2+2] cycloaddition reactions of enediynes **3** and **4**.

 © 2011 Wiley-VCH Verlag GmbH & Co. KGaA, Weinheim

1,6,11,16-Tetrakis(4-methylphenylsulfonyl)-1,6,11,16-tetraazahexadeca-3-ene-8,13-diyne (4): A mixture of **3** (0.30 g, 0.32 mmol), trifluoroacetic acid (1.5 mL) and dichloromethane (4 mL) was stirred at room temperature for 3 h (TLC monitoring). The liquid was distilled off under vacuum and the residue was dissolved in ethyl acetate (20 mL). The organic layer was subsequently washed with aqueous sodium bicarbonate (3×20 mL), H_2O (3×20 mL) and brine (20 mL), dried (Na_2SO_4) and filtered. The solvent was evaporated under reduced pressure to afford **4** (0.23 g, 96%) as a colourless solid. M.p. 70–74°C; ^{1}H NMR (200 MHz, $CDCl_3$, 25°C, TMS): δ=2.43 (s, 6H), 2.45 (s, 6H), 3.52 (m, 4H), 3.65 (d, ^3J(H,H)= 6 Hz, 2H), 3.82 (m, 4H), 3.91 (s, 2H), 4.89 (t, ^3J(H,H)=5.2 Hz, 2H), 5.55 (m, 2H), 7.31 (m, 8H), 7.62 (AA′BB′ system, ^3J(H,H)=8.4 Hz, 2H), 7.66 (AA′BB′ system, ^3J(H,H)=8.4 Hz, 2H), 7.70 (AA′BB′ system, ^3J(H,H)= 8.2 Hz, 2H), 7.72 ppm (AA′BB′ system, ^3J(H,H)=8.2 Hz, 2H); ^{13}C NMR (50 MHz, $CDCl_3$, 25°C, TMS): δ=21.5, 32.8, 36.3, 36.4, 36.5, 44.4, 48.2, 126.9, 127.1, 127.2, 127.6, 127.9, 129.6, 129.7, 129.8, 130.9, 135.1, 135.7, 136.4, 136.7, 143.6, 143.9, 144.0, 144.2 ppm; IR (ATR): $\tilde{\nu}$=3283, 2922, 1326, 1154 cm^{-1}; HRMS (ESI): *m/z* calcd for $C_{40}H_{44}N_4S_4O_8$+Na^+: 859.1934; found: 859.1897.

General method for the cycloaddition reactions of 1–4: A degassed solution of enediyne (0.05 mmol) and chlorotris(triphenylphosphane) rhodium(I) (0.005 mmol, 10% molar) in anhydrous toluene (10 mL) was heated (temperatures and reaction times specified in Table 1) until completion (TLC monitoring). The solvent was then evaporated and the residue was purified by column chromatography on silica gel.

Cyclohexadiene 10: Column chromatography: from hexanes/dichloromethane (7:3) to hexanes/dichloromethane/ethyl acetate (7:3:1) to afford **10** (0.03 g, 55%) as a colourless solid. M.p. 90–93°C; ^{1}H NMR (600 MHz, [D_6]DMSO, 25°C): δ=1.31 (s, 18H), 2.38 (s, 6H), 2.39 (s, 6H), 2.41 (m, 2H), 2.55 (m, 2H), 3.69 (d, ^3J(H,H)=15 Hz, 2H), 3.77 (m, 2H), 4.00 (d, ^3J(H,H)=15 Hz, 2H), 4.43 (d, ^3J(H,H)=16.2 Hz, 2H), 4.50 (d, ^3J(H,H)= 16.2 Hz, 2H), 7.38 (AA′BB′ system, ^3J(H,H)=7.8 Hz, 4H), 7.43 (AA′BB′ system, ^3J(H,H)=7.8 Hz, 4H), 7.63 (AA′BB′ system, ^3J(H,H)=8.4 Hz, 4H), 7.66 ppm (AA′BB′ system, ^3J(H,H)=8.4 Hz, 4H); ^{13}C NMR (150 MHz, [D_6]DMSO, 25°C): δ=21.0, 27.1, 42.7, 44.6, 49.1, 52.4, 125.4, 127.3, 127.6, 129.5, 129.8, 131.8, 136.0, 136.2, 143.7, 144.7, 150.3 ppm; IR (ATR): $\tilde{\nu}$=2921, 1727, 1347, 1153 cm^{-1}; HRMS (ESI): *m/z* calcd for $C_{50}H_{60}N_4S_4O_{12}$+Na^+: 1059.2983; found: 1059.2944; *m/z* calcd for $C_{50}H_{60}N_4S_4O_{12}$+K^+: 1075.2722; found: 1075.2685.

Cyclohexadiene 11: Column chromatography: from hexanes/dichloromethane/ethyl acetate (5:3:1) to hexanes/dichloromethane/ethyl acetate (7:3:2) to afford **11** (0.04 g, 85%) as a colourless solid. M.p. 106–108°C; ^{1}H NMR (600 MHz, [D_6]DMSO, 25°C): δ=1.35 (m, 2H), 2.11 (m, 2H), 2.27 (s, 6H), 2.44 (s, 6H), 3.37 (m, 2H), 3.40 (m, 2H), 3.60 (d, ^3J(H,H)= 15 Hz, 2H), 3.68 (dd, ^3J(H,H)=6 Hz, ^2J(H,H)=15 Hz, 2H), 3.85 (d, ^2J-(H,H)=15 Hz, 2H), 7.07 (AA′BB′ system, ^3J(H,H)=8.4 Hz, 4H), 7.20 (AA′BB′ system, ^3J(H,H)=8.4 Hz, 4H), 7.55 (AA′BB′ system, ^3J(H,H)= 8.4 Hz, 4H), 7.67 (AA′BB′ system, ^3J(H,H)=8.4 Hz, 4H), 7.74 ppm (t, ^3J-(H,H)=6 Hz, 2H); ^{13}C NMR (150 MHz, [D_6]DMSO, 25°C): δ=20.7, 21.0, 39.8, 41.1, 48.7, 52.7, 124.1, 125.9, 128.5, 129.0, 129.9, 132.0, 136.9, 138.5, 142.4, 143.9 ppm; IR (ATR): $\tilde{\nu}$=3282, 2922, 1324, 1153 cm^{-1}; HRMS (ESI): *m/z* calcd for $C_{40}H_{44}N_4S_4O_8$+Na^+: 859.1934; found: 859.1899.

Cyclohexadiene 14: Column chromatography: from hexanes/dichloromethane (6:4) to hexanes/dichloromethane/ethyl acetate (6:4:1) to afford **14** (0.03 g, 65%) as a colourless solid. M.p. 97–101°C; ^{1}H NMR (600 MHz, [D_6]DMSO, 25°C): δ=1.30 (s, 9H), 2.27 (s, 3H), 2.33 (s, 3H), 2.35–2.40 (m, 1H), 2.35–2.40 (m, 1H), 2.42 (s, 3H), 2.45 (s, 3H), 2.50–2.51 (m, 1H), 3.28–3.30 (m, 1H), 3.45 (dd, ^3J(H,H)=5.4 Hz, ^2J(H,H)=14.4 Hz, 1H), 3.61 (app d, ^2J(H,H)=16.8 Hz, 1H), 3.79 (m, 1H), 3.81–3.83 (m, 1H), 3.85–3.87 (m, 3H), 3.90 (app d, ^2J(H,H)=16.8 Hz, 2H), 4.09–4.11 (m, 1H), 7.28 (BB′ system, ^3J(H,H)=7.8 Hz, 2H), 7.30 (BB′ system, ^3J-(H,H)=7.8 Hz, 2H), 7.47 (BB′ system, ^3J(H,H)=7.8 Hz, 2H), 7.50 (BB′ system, ^3J(H,H)=7.8 Hz, 2H), 7.54 (AA′ system, ^3J(H,H)=8.4 Hz, 2H), 7.57 (t, ^3J(H,H)=6 Hz, 1H), 7.65 (AA′ system, ^3J(H,H)=8.4 Hz, 2H), 7.66 (AA′ system, ^3J(H,H)=7.8 Hz, 2H), 7.81 ppm (AA′ system, ^3J-(H,H)=7.8 Hz, 2H); ^{13}C NMR (150 MHz, [D_6]DMSO, 25°C): δ=20.9, 21.0, 30.0, 41.0, 42.0, 43.2, 48.2, 49.8, 50.2, 54.9, 84.5, 122.2, 124.3, 126.6, 127.5, 128.6, 129.4, 129.6, 129.7, 132.0, 132.2, 133.5, 136.3, 137.2, 142.7, 143.8, 144.7, 150.7, 166.9 ppm; IR (ATR): $\tilde{\nu}$=3321, 2920, 1728, 1346, 1157 cm^{-1}; HRMS (ESI): *m/z* calcd for $C_{45}H_{52}N_4S_4O_{10}$+Na^+: 959.2458; found: 959.2413.

Cyclohexadiene 15: Column chromatography: hexanes/dichloromethane/ethyl acetate (5:3:2) to afford **15** (0.05 g, 89%) as a colourless solid. M.p. 107–109°C; ^{1}H NMR (600 MHz, $CDCl_3$, 25°C, TMS): δ=1.86 (d, ^3J-(H,H)=16.0 Hz, 1H), 2.17 (s, 3H), 2.30 (t, ^3J(H,H)=9.9 Hz, 1H), 2.37 (s, 3H), 2.40 (s, 3H), 2.41 (s, 3H), 2.69–2.73 (m, 2H), 3.09 (m, 1H), 3.26 (dd, ^3J(H,H)=5.0 Hz, ^2J(H,H)=15.0 Hz, 1H), 3.48 (m, 1H), 3.55 (d, ^2J-(H,H)=15.5 Hz, 1H), 3.70–3.80 (m, 3H), 3.84 (t, J=8.8 Hz, 1H), 3.90–3.93 (m, 2H) , 7.17 (d, ^3J(H,H)=8.0 Hz, 2H), 7.37 (br s, 1H), 7.38 (d, ^3J-(H,H)=8.0 Hz, 2H), 7.41 (d, ^3J(H,H)=8.0 Hz, 4H), 7.45 (d, ^3J(H,H)= 8.0 Hz, 2H), 7.58 (t, ^3J(H,H)=5.3 Hz, 1H), 7.67–7.70 ppm (m, 6H); ^{13}C NMR (150 MHz, $CDCl_3$, 25°C, TMS): δ=21.6, 21.9, 21.9, 21.9, 40.8, 41.6, 41.8, 42.7, 49.6, 50.0, 50.7, 54.7, 123.6, 124.3, 127.2, 127.4, 128.5, 128.6, 128.7, 130.1, 130.5, 130.7, 130.8, 132.7, 133.3, 134.3, 138.3, 138.3, 143.5, 143.6, 144.6, 144.6 ppm; IR (ATR): $\tilde{\nu}$=3296, 2926, 1333, 1157 cm^{-1}; HRMS (ESI): *m/z* calcd for $C_{40}H_{44}N_4S_4O_8$+Na^+: 859.1934; found: 859.1934; *m/z* calcd for $C_{40}H_{44}N_4S_4O_8$+K^+: 875.1674; found: 875.1681.

Computational methods: All geometry optimisations were performed by using the hybrid DFT B3LYP[20] method with the Gaussian03[21] program package. The geometry optimisations were performed without symmetry constraints. Analytical Hessians were computed to determine the nature of the stationary points (one or zero imaginary frequencies for transition states and minima, respectively) and to calculate unscaled zero-point energies (ZPEs), as well as thermal corrections and entropy effects using the standard statistical mechanics relationships for an ideal gas.[22] These two latter terms were computed at 298.15 K and 1 atm to provide the relative Gibbs energies (ΔG_{298}). Furthermore, the connectivity between stationary points was established by calculations of the intrinsic reaction paths.[23] The all-electron cc-pVDZ basis set was used for phosphorus, oxygen, nitrogen, carbon, and hydrogen atoms,[24] whereas for rhodium we employed the cc-pVDZ-PP basis set[25] containing an effective core relativistic pseudopotential. Relative energies were computed by taking into account the total number of molecules present. The SO_2Ar moieties present in the experimental enediynes and the phenyl group in the catalyst were substituted by hydrogen atoms to reduce the computational complexity of the calculations involving these ligands. Substitution of PPh_3 by PH_3 is a common procedure in theoretical organometallic chemistry.[26,27] In addition, we have checked that, despite the electronic and steric differences, substitution of PPh_3 by PH_3 does not introduce significant changes in the thermodynamics and kinetics of the cycloaddition of three acetylene molecules.[14] A previous study found that solvent effects due to toluene and acetonitrile in [2+2+2] cycloadditions are minor, likely due to the absence of charged or polarised intermediates and transition states in the reaction mechanism.[28] Because the reactions studied were carried out in toluene, solvent effects have not been included in the present calculations. Finally, because there are no experimental data suggesting the presence of paramagnetic intermediates, our studies were limited to the singlet potential energy surfaces.

Acknowledgements

Financial support from the Spanish MICINN (CTQ2008-05409-C02-02, CTQ2008-03077, CTQ2011-23156, CTQ2011-23121 and CTQ2009-08328) and the Catalan DIUE of the Generalitat de Catalunya (2009SGR637) is acknowledged. A.D. thanks the Spanish MEC for a doctoral fellowship. Support for the research of M.S. was received through the ICREA Academia 2009 prize for excellence in research funded by the DIUE. We also acknowledge the Centre de Serveis Científics i Acadèmics de Catalunya (CESCA) for partial funding of computer time.

[1] For reviews, see: a) K. P. C. Vollhardt, *Angew. Chem.* **1984**, *96*, 525; *Angew. Chem. Int. Ed. Engl.* **1984**, *23*, 539; b) M. Lautens, W. Klute,

 © 2011 Wiley-VCH Verlag GmbH & Co. KGaA, Weinheim

W. Tam, *Chem. Rev.* **1996**, *96*, 49; c) P. R. Chopade, J. Louie, *Adv. Synth. Catal.* **2006**, *348*, 2307; d) V. Gandon, C. Aubert, M. Malacria, *Chem. Commun.* **2006**, 2209; e) G. Domínguez, J. Pérez-Castells, *Chem. Soc. Rev.* **2011**, *40*, 3430.

[2] For selected references involving two alkynes and one alkene, see: a) D. W. Macomber, A. G. Verma, R. D. Rogers, *Organometallics* **1988**, *7*, 1241; b) S.-I. Ikeda, N. Mori, Y. Sato, *J. Am. Chem. Soc.* **1997**, *119*, 4779; c) N. Mori, S.-I. Ikeda, Y. Sato, *J. Am. Chem. Soc.* **1999**, *121*, 2722; d) V. Gandon, D. Leboeuf, S. Amslinger, K. P. C. Vollhardt, M. Malacria, C. Aubert, *Angew. Chem.* **2005**, *117*, 7276; *Angew. Chem. Int. Ed.* **2005**, *44*, 7114; e) G. Hilt, A. Paul, K. Harms, *J. Org. Chem.* **2008**, *73*, 5187; f) Y. Obora, Y. Satoh, Y. Ishii, *J. Org. Chem.* **2010**, *75*, 6046; for selected references involving diynes and alkenes, see: g) Y. Wakatsuki, T. Kuramitsu, H. Yamazaki, *Tetrahedron Lett.* **1974**, *15*, 4549; h) H. Suzuki, K. Itoh, Y. Ishii, K. Simon, J. A. Ibers, *J. Am. Chem. Soc.* **1976**, *98*, 8494; i) Z. Zhou, L. P. Battaglia, G. P. Chiusoli, M. Costa, M. Nardelli, C. Pelizzi, G. Predieri, *J. Chem. Soc. Chem. Commun.* **1990**, 1632; j) Z. Zhou, M. Costa, G. P. Chiusoli, *J. Chem. Soc. Perkin Trans. 1* **1992**, 1399; k) E. S. Johnson, G. J. Balaich, I. P. Rothwell, *J. Am. Chem. Soc.* **1997**, *119*, 7685; l) Y. Yamamoto, H. Kitahara, R. Hattori, K. Itoh, *Organometallics* **1998**, *17*, 1910; m) T.-Y. Hsiao, K. C. Santhosh, K.-F. Liou, C.-H. Chen, *J. Am. Chem. Soc.* **1998**, *120*, 12232; n) Y. Yamamoto, H. Kitahara, R. Ogawa, K. Itoh, *J. Org. Chem.* **1998**, *63*, 9610; o) S.-I. Ikeda, H. Watanabe, Y. Sato, *J. Org. Chem.* **1998**, *63*, 7026; p) T. Sambaiah, L.-P. Li, D.-J. Huang, C.-H. Lin, D. K. Rayabarapu, C.-H. Cheng, *J. Org. Chem.* **1999**, *64*, 3663; q) Y. Yamamoto, H. Kitahara, R. Ogawa, H. Kawaguchi, K. Tatsumi, K. Itoh, *J. Am. Chem. Soc.* **2000**, *122*, 4310; r) T. Sambaiah, D.-J. Huang, C.-H. Cheng, *J. Chem. Soc. Perkin Trans. 1* **2000**, 195; s) M. J. Sung, J.-H. Pang, S.-B. Park, J. K. Cha, *Org. Lett.* **2003**, *5*, 2137; t) Y. Yamamoto, S. Kuwabara, Y. Ando, H. Nagata, H. Nishiyama, K. Itoh, *J. Org. Chem.* **2004**, *69*, 6697; u) M.-S. Wu, D. K. Rayabarapu, C.-H. Cheng, *Tetrahedron* **2004**, *60*, 10005; v) S. Kezuka, S. Tanaka, T. Ohe, Y. Nakaya, R. Takeuchi, *J. Org. Chem.* **2006**, *71*, 543; w) C. Aubert, V. Gandon, S. Han, B. M. Johnson, M. Malacria, S. Schömenauer, K. P. C. Vollhardt, G. D. Whitener, *Synthesis* **2010**, 2179.

[3] For selected references involving enynes and alkynes, see: a) S. Kezuka, T. Okado, E. Niou, R. Takeuchi, *Org. Lett.* **2005**, *7*, 1711; for selected references involving enediynes, see: b) E. D. Sternberg, K. P. C. Vollhardt, *J. Org. Chem.* **1982**, *47*, 3447; c) F. Slowinski, C. Aubert, M. Malacria, *Tetrahedron Lett.* **1999**, *40*, 707; d) F. Slowinski, C. Aubert, M. Malacria, *Tetrahedron Lett.* **1999**, *40*, 5849; e) F. Slowinski, C. Aubert, M. Malacria, *Adv. Synth. Catal.* **2001**, *343*, 64; f) F. Slowinski, C. Aubert, M. Malacria, *Eur. J. Org. Chem.* **2001**, 3491; g) F. Slowinski, C. Aubert, M. Malacria, *J. Org. Chem.* **2003**, *68*, 378; h) P. Eckenberg, U. Groth, *Synlett* **2003**, 2188; i) Ref. [2p]; j) M. Schelper, O. Buisine, S. Kozhuskov, C. Aubert, A. de Meijere, M. Malacria, *Eur. J. Org. Chem.* **2005**, 3000; k) A. Geny, S. Gaudrel, F. Slowinski, M. Amatore, G. Chouraqui, M. Malacria, C. Aubert, V. Gandon, *Adv. Synth. Catal.* **2009**, *351*, 271.

[4] a) R. Grigg, R. Scott, P. Stevenson, *J. Chem. Soc. Perkin Trans. 1* **1988**, 1365; b) C. H. Oh, H. R. Sung, S. H. Jung, Y. M. Lim, *Tetrahedron Lett.* **2001**, *42*, 5493; c) P. A. Evans, J. R. Sawyer, K. W. Lai, J. C. Huffman, *Chem. Commun.* **2005**, 3971; d) A. Torrent, I. González, A. Pla-Quintana, A. Roglans, M. Moreno-Mañas, T. Parella, J. Benet-Buchholz, *J. Org. Chem.* **2005**, *70*, 2033; e) B. Bennacer, M. Fijiwara, S.-Y. Lee, I. Ojima, *J. Am. Chem. Soc.* **2005**, *127*, 17756; f) I. González, S. Bouquillon, A. Roglans, J. Muzart, *Tetrahedron Lett.* **2007**, *48*, 6425; g) S. Brun, L. Garcia, I. González, A. Torrent, A. Dachs, A. Pla-Quintana, T. Parella, A. Roglans, *Chem. Commun.* **2008**, 4339; h) L. X. Alvarez, B. Bessières, J. Einhorn, *Synlett* **2008**, 1376; i) A. L. Jones, J. K. Snyder, *J. Org. Chem.* **2009**, *74*, 2907.

[5] a) K. Tsuchikama, Y. Kuwata, T. Shibata, *J. Am. Chem. Soc.* **2006**, *128*, 13686; b) T. Shibata, A. Kawachi, M. Ogawa, Y. Kuwata, K. Tsuchikama, K. Endo, *Tetrahedron* **2007**, *63*, 12853; c) M. Kobayashi, T. Suda, K. Noguchi, K. Tanaka, *Angew. Chem. Int. Ed.* **2011**, *50*, 1664.

[6] a) P. A. Evans, K. W. Lai, J. R. Sawyer, *J. Am. Chem. Soc.* **2005**, *127*, 12466; b) T. Shibata, Y. Arai, Y. Tahara, *Org. Lett.* **2005**, *7*, 4955; c) T. Shibata, M. Otomo, Y.-k. Tahara, K. Endo, *Org. Biomol. Chem.* **2008**, *6*, 4296.

[7] a) T. Shibata, H. Kurokawa, K. Kanda, *J. Org. Chem.* **2007**, *72*, 6521; b) K. Tanaka, G. Nishida, H. Sagae, M. Hirano, *Synlett* **2007**, 1426; c) Ref. [4g]; d) S. Brun, M. Parera, A. Pla-Quintana, A. Roglans, T. León, T. Achard, J. Solà, X. Verdaguer, A. Riera, *Tetrahedron* **2010**, *66*, 9032.

[8] a) J. A. Varela, S. G. Rubín, C. González-Rodríguez, L. Castedo, C. Saá, *J. Am. Chem. Soc.* **2006**, *128*, 9262; b) J. A. Varela, S. García-Rubín, L. Castedo, C. Saá, *J. Org. Chem.* **2008**, *73*, 1320; c) S. García-Rubín, J. A. Varela, L. Castedo, C. Saá, *Chem. Eur. J.* **2008**, *14*, 9772; d) J. A. Varela, C. Saá, *J. Organomet. Chem.* **2009**, *694*, 143.

[9] a) D. Leboeuf, L. Iannazzo, A. Geny, M. Malacria, K. P. C. Vollhardt, C. Aubert, V. Gandon, *Chem. Eur. J.* **2010**, *16*, 8904; b) V. Gandon, N. Agelet, K. P. C. Vollhardt, M. Malacria, C. Aubert, *J. Am. Chem. Soc.* **2006**, *128*, 8509.

[10] See footnote 20 in: Y. Shibata, Y. Otake, M. Hirano, K. Tanaka, *Org. Lett.* **2009**, *11*, 689.

[11] J. J. Kaloko, Y-H. G. Teng, I. Ojima, *Chem. Commun.* **2009**, 4569.

[12] a) A. Pla-Quintana, A. Roglans, A. Torrent, M. Moreno-Mañas, J. Benet-Buchholz, *Organometallics* **2004**, *23*, 2762; b) S. Cerezo, J. Cortés, D. Galvan, E. Lago, C. Marchi, E. Molins, M. Moreno-Mañas, R. Pleixats, J. Torrejón, A. Vallribera, *Eur. J. Org. Chem.* **2001**, 329.

[13] A. Dachs, S. Osuna, A. Roglans, M. Solà, *Organometallics* **2010**, *29*, 562.

[14] For the cycloaddition of three acetylene molecules catalysed by $[RhCl(PR_3)_3]$, the reaction energy is $-134.5\ kcal\,mol^{-1}$ for both R = H and Ph, whereas the Gibbs energy barrier for the rate-determining step is 19.8 and $24.7\ kcal\,mol^{-1}$ for R = H and Ph, respectively (see Ref. [13]).

[15] A. Dachs, A. Torrent, A. Roglans, T. Parella, S. Osuna, M. Solà, *Chem. Eur. J.* **2009**, *15*, 5289.

[16] A. Dachs, A. Roglans, M. Solà, *Organometallics* **2011**, *30*, 3151.

[17] Indeed, at the same level of theory, substitution of two phosphine ligands by acetylene molecules in $[RhCl(PPh_3)_3]$ is exoergonic by about $6\ kcal\,mol^{-1}$, whereas in $[RhCl(PH_3)_3]$ it is endoergonic by $11\ kcal\,mol^{-1}$ (see Ref. [13]).

[18] a) W. Scherer, G. S. McGrady, *Angew. Chem.* **2004**, *116*, 1816; *Angew. Chem. Int. Ed.* **2004**, *43*, 1782; b) T. S. Thakur, G. R. Desiraju, *J. Mol. Struct. THEOCHEM* **2007**, *810*, 143.

[19] L. Jiao, M. Lin, Z.-X. Yu, *J. Am. Chem. Soc.* **2011**, *133*, 447.

[20] a) A. D. Becke, *J. Chem. Phys.* **1993**, *98*, 5648; b) C. Lee, W. Yang, R. G. Parr, *Phys. Rev. B* **1988**, *37*, 785; c) P. J. Stephens, F. J. Devlin, C. F. Chabalowski, M. J. Frisch, *J. Phys. Chem.* **1994**, *98*, 11623.

[21] Gaussian 03, Revision C.01, M. J. Frisch, G. W. Trucks, H. B. Schlegel, G. E. Scuseria, M. A. Robb, J. R. Cheeseman, J. A. Montgomery, Jr., T. Vreven, K. N. Kudin, J. C. Burant, J. M. Millam, S. S. Iyengar, J. Tomasi, V. Barone, B. Mennucci, M. Cossi, G. Scalmani, N. Rega, G. A. Petersson, H. Nakatsuji, M. Hada, M. Ehara, K. Toyota, R. Fukuda, J. Hasegawa, M. Ishida, T. Nakajima, Y. Honda, O. Kitao, H. Nakai, M. Klene, X. Li, J. E. Knox, H. P. Hratchian, J. B. Cross, V. Bakken, C. Adamo, J. Jaramillo, R. Gomperts, R. E. Stratmann, O. Yazyev, A. J. Austin, R. Cammi, C. Pomelli, J. W. Ochterski, P. Y. Ayala, K. Morokuma, G. A. Voth, P. Salvador, J. J. Dannenberg, V. G. Zakrzewski, S. Dapprich, A. D. Daniels, M. C. Strain, O. Farkas, D. K. Malick, A. D. Rabuck, K. Raghavachari, J. B. Foresman, J. V. Ortiz, Q. Cui, A. G. Baboul, S. Clifford, J. Cioslowski, B. B. Stefanov, G. Liu, A. Liashenko, P. Piskorz, I. Komaromi, R. L. Martin, D. J. Fox, T. Keith, M. A. Al-Laham, C. Y. Peng, A. Nanayakkara, M. Challacombe, P. M. W. Gill, B. Johnson, W. Chen, M. W. Wong, C. Gonzalez, J. A. Pople, Gaussian, Inc., Wallingford CT, **2004**.

[22] P. Atkins, J. De Paula, *Physical Chemistry*, 8th ed., Oxford University Press, Oxford, **2006**.

[23] C. Gonzalez, H. B. Schlegel, *J. Chem. Phys.* **1989**, *90*, 2154.

 © 2011 Wiley-VCH Verlag GmbH & Co. KGaA, Weinheim

[24] a) T. H. Dunning, Jr., *J. Chem. Phys.* **1989**, *90*, 1007; b) D. E. Woon, T. H. Dunning, Jr., *J. Chem. Phys.* **1993**, *98*, 1358.
[25] K. A. Peterson, D. Figgen, M. Dolg, H. Stoll, *J. Chem. Phys.* **2007**, *126*, 124101.
[26] a) J. H. Hardesty, J. B. Koerner, T. A. Albright, G.-Y. Lee, *J. Am. Chem. Soc.* **1999**, *121*, 6055; b) L. F. Veiros, G. Dazinger, K. Kirchner, M. J. Calhorda, R. Schmid, *Chem. Eur. J.* **2004**, *10*, 5860.
[27] a) Q. Cui, D. G. Musaev, K. Morokuma, *Organometallics* **1997**, *16*, 1355; b) Q. Cui, D. G. Musaev, K. Morokuma, *Organometallics* **1998**, *17*, 742; c) Q. Cui, D. G. Musaev, K. Morokuma, *Organometallics* **1998**, *17*, 1383; d) W. Zheng, A. Ariafard, Z. Lin, *Organometallics* **2008**, *27*, 246; e) Y. Abe, K. Kuramoto, M. Ehara, H. Nakatsuji, M. Suginome, M. Murakami, Y. Ito, *Organometallics* **2008**, *27*, 1736.
[28] L. Orian, J. N. P. van Strale, F. M. Bickelhaupt, *Organometallics* **2007**, *26*, 3816.

Received: July 19, 2011
Published online: November 23, 2011

 © 2011 Wiley-VCH Verlag GmbH & Co. KGaA, Weinheim